BIO-3910

MASTER'S THESIS IN BIOLOGY

The substrate specificities and physiological function of the *Toxoplasma gondii* apicoplast phosphate translocator

Hanne Risan Johnsen

May, 2009

FACULTY OF SCIENCE
Department of Biology

University of Tromsø

BIO-3910

MASTER'S THESIS IN BIOLOGY

The substrate specificities and physiological function of the *Toxoplasma gondii* apicoplast phosphate translocator

Hanne Risan Johnsen

May, 2009

Table of contents

Acknowledgments

I would like to express my gratitude to my supervisor professor Karsten Fischer who gave me the opportunity to work on this project and for guiding me throughout the process. Thanks to all the people at the Department of Biology at the University of Tromsø for support and friendship. A special thank to Rafal Butowt which I have cooperated with in this project.

Most of the work presented in this thesis was carried out at the AG Flügge lab at Botanisches Institut, Köln. I would like to give a special thanks to professor Ulf-Ingo Flügge and his working group for their hospitality. Thanks to Sonja Hetfeld and Diana Hille for guiding me in the laboratory.

I must acknowledge the kind offer of TgPT cDNA from Dr. Wolfgang Bohne and his group at the Institute of Medical Microbiology, University of Göttingen.

Lastly, I would like to thank friends and family for their support!

Abbreviations

3-PGA	3-phosphoglycerate
ATP	Adenosine Triphosphate
Bp	Base pairs
cDNA	complementary DNA
dH_2O	distilled water
DOXP	1-deoxy-D-xylulose 5- phosphate
F	Farad
FAS	Fatty Acid Synthesis
G	Gravity in centrifugation
GAPDH	Glyceraldehyde 3-phosphate Dehydrogenase
GPI	Glucose-6-phsophate Isomerase
GPT	Glucose-6-phosphate Translocator
His	Histidin
kV	kilo Volt
LB	Luria Bertani
MVA	Mevalonate
NADH	Nicotinamide Adenine Dinucleotide
OPPP	Oxidative Pentose Phosphate Pathway
PCR	Polymerase Chain Reaction
PDH	Pyruvate Dehydrogenase Complex
PEP	Phosphoenolpyruvate
P_i	Inorganic phosphate
PPT	Phosphoenolpyruvate/ Phosphate Translocator
pPT	plastidic Phosphate Translocator
rpm	revolutions per minute
SC	Synthetic Complete
SDS-PAGE	Sodium Dodecyl Sulfate Polyacrylamide Gel Electrophoresis
TgPT	*Toxoplasma gondii* Phosphate Translocator
TP	Triose Phosphates
TPT	Triose Phosphate Translocator
XPT	Xylulose-5-phosphate Translocator
Xyl5P	Xylulose-5-phosphate

Abstract

The apicomplexan parasites including the causative agents of malaria (*Plasmodium* spp.) and toxoplasmosis (*Toxoplasma gondii*) are running the risk of developing resistance to existing drugs. Members of the phylum Apicomplexa harbour a relict plastid, the apicoplast, which show homology to the chloroplasts of plants and algae. The apicoplast appears to be indispensable to the parasites, and due to its prokaryotic origin it represents an excellent drug target. *T. gondii* possesses a single plastidic membrane transporter (TgPT) that shows similarity to the phosphate translocators (pPTs) in higher plants which comprises four subfamilies (TPT, PPT, GPT, XPT). Its physiological function has not been previously studied, but the TgPT was proposed to comprise a connection between the metabolic pathways in the apicoplast and the metabolic processes in the cytosol. In this study, the substrate specificities of the TgPT were determined by heterologous expression of the protein in yeast and reconstitution of its transport activity in liposomes. The TgPT showed similarities to both TPTs and PPTs from higher plants combining the transport activities of the two subfamilies by simultaneously transporting compounds phosphorylated at different C-atoms. The TgPT accepts inorganic phosphate and PEP equally as substrates, having an even higher affinity to triose phosphates and 3-PGA. Based on our results, the TgPT likely connect the cytosolic metabolism with metabolic pathways in the apicoplast by delivering carbon units for at least two essential biosynthetic pathways, the fatty acid synthesis and the DOXP pathway for isoprenoid synthesis. Additionally, the TgPT contributes an indirect supply of ATP and reduction power to the apicoplast. These results have recently been corroborated by Boris Striepen and his group by showing that a knock-out of the TgPT resulted in rapid death of the parasite, establishing the transporter as essential for parasite viability and thereby an attractive drug target.

1. Introduction

1.1 Phylum Apicomplexa

Apicomplexan parasites represent a large phylum consisting of several thousands of protozoan species including the causative agents of malaria (*Plasmodium* spp.) and toxoplasmosis (*Toxoplasma gondii*) (Levine 1988). Because of an emerging resistance in the apicomplexan parasites to the already existing drugs there is an urgent need for new treatments as well as new targets in the fight against malaria, toxoplasmosis and other parasitic diseases (Trape *et al.* 2002).

Malaria is one of the world's major diseases found in many tropical and subtropical regions. Of the four species of *Plasmodium* that infects humans, *Plasmodium falciparum* is the most lethal. The disease is transmitted to humans by infected female mosquitoes that inject saliva together with an anticoagulant during blood feeding. Saliva from an infected mosquito contains motile asexual cells, sporozoites, which are transported with the blood to the liver where they divide asexually and produces daughter cells, merozoites. Released merozoites invade red blood cells where they enlarge and turn into a ring-formed feeding stage, trophozoites, which split again to form a multinucleated cell stage, schizonts, that produce large amounts of new merozoites. When the merozoites are released into the body the host displays the flu-like symptoms of malaria. The symptoms may appear and disappear in phases, these cyclic symptoms of malaria are caused by the life cycle of the parasites, as they develop, mature, reproduce and are once again released into the blood stream to infect new cells. Some of the merozoites reach the sexual phase and turn into gametocytes that start to produce gametes only when extracted from the infected human host by a mosquito (Wiesner 2003).

T. gondii has a complex lifecycle that alternates between asexually dividing forms and a sexual phase. The asexual part of the life cycle can take place in any warm-blooded animal, including humans, causing the disease toxoplasmosis. Humans acquire toxoplasmosis by contact with infected cat feces or by ingestion of undercooked and raw meat. It is estimated that about one-third of the world's human population are infected with *Toxoplasma*, but the infection is usually asymptomatic in healthy individuals. Toxoplasmosis is the most common opportunistic infection in immunocompromised patients with AIDS or in transplant patients (Luft and Remington 1988). In addition, congenital transmission can occur if woman are infected with *Toxoplasma* for the first time during pregnancy (Kim and Weiss 2008). The sexual part of the life cycle takes place only in members of the family *Felidae,* including wild and domestic cats. Cats may become infected with *T. gondii* either by ingestion of infectious oocysts from the environment or by ingestion of tissue cysts from intermediate hosts as rodents and birds (Tenter *et al.* 2000). The transmission of the parasite can be facilitated by its ability to modify its host's behavior. Infection with *T.gondii* in rats alters their perception of cats, in some cases even turning their natural aversion into attraction (Berdoy 2000).

The basic biochemistry, genetics, and subcellular architecture of the apicomplexan species are prominently similar, although many aspects of disease pathogenesis, host range and life cycle are not conserved. *T. gondii,* being the most experimentally tractable, has been used as a model system for studying many biological aspects of apicomplexan parasites (David *et al.* 2002, Pfefferkorn *et al.* 1988). *T. gondii* provides an attractive experimental system as the parasite can be grown in many different cell types (Pfefferkorn *et al.* 1988), and most organelles can be labeled with fluorescent reporters permitting quantitative analysis in living cells (Striepen *et al*. 1998, 2000). Ultrastructural studies have revealed a detailed picture of the *T. gondii* cell structure (Hager *et al.* 1999), and the cells can be stably transformed both by homologous and non-homologous transformation (Roos *et al.* 1994).

1.2 The apicoplast

Plastids are plant-specific organelles which are able to perform many specialized functions that are essential for plant growth and development, such as photosynthesis, nitrogen assimilation, synthesis of amino acids and fatty acids, as well as storage of carbohydrates and lipids (Bowsher *et al.* 1992). Even in non-photosynthetic plants and algae the plastids are indispensable because cells containing plastids have become dependent on certain metabolic pathways for the production of metabolites that are exported from the organelle (McFadden and Roos 1999, Ralph *et al.* 2001).

Members of the phylum Apicomplexa hold a relict plastid, homologous to the chloroplast of plants and algae. The apicoplast is a four-membrane-bound compartment, distinct from the mitochondria and other organelles, which was first identified in *T. gondii* by *in situ* hybridization experiments. The organelle contains a 35-kb circular genome that encodes a number of genes including RNA polymerase and ribosomal genes (Kohler *et al.* 1997, McFadden *et al.* 1996, Wilson *et al.* 1996). The sequencing of the full *P. falciparum* genome and the identification of an apicoplast-targeting sequence (Foth *et al.* 2003) allowed identification of several hundred nuclear-encoded proteins that probably are targeted to this organelle, including housekeeping enzymes involved in DNA replication, transcription, translation, protein import, and specific metabolic and transport activities (Gardner *et al.* 2002).

All plastids have originated from a primary endosymbiosis where photosynthetic prokaryotes were engulfed by phagotrophic eukaryotes (Cavalier-Smith 1982). This event led to the development of red and green algae, plants and glaucophytes by the production of a double membrane bound endosymbiont that subsequently became a chloroplast. A further engulfment of the primary endosymbionts by other phagotrophic eukaryotes resulted in a lateral transfer of the plastid into several eukaryotic lineages. Secondary endosymbiosis has occurred several times and by preservation of the plastid it has given rise to diverse groups of algae and other eukaryotes (McFadden and Gilson 1995, McFadden and Roos 1999).

Both the phylogeny of the apicoplast genome and the structure of the organelle support that the plastid evolved through secondary endosymbiosis (McFadden and Roos 1999). One of the characteristics for secondary plastids is the presence of more than two membranes surrounding the organelle. The apicoplast has four membranes (Illustrated in figure 1) (Kohler *et al.* 1997) whereas two are presumed to be derived from the chloroplast, one from the algae plasma membrane and one from the host cell (Fast *et al.* 2001).

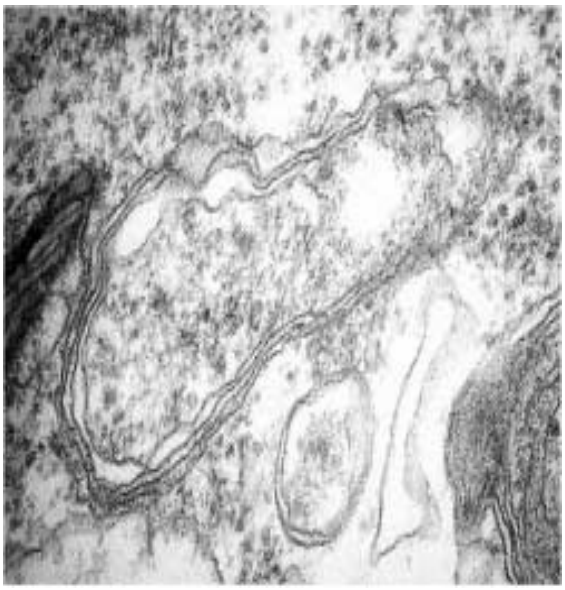

Figure 1: The four membranes surrounding the apicoplast. Show a transmission electron micrograph of a *Plasmodium* apicoplast with four membranes (Figure from Ralph *et al.* 2004). Secondary plastids have one or two additional membranes from the engulfment of a primary plastid-containing eukaryote by a second eukaryote.

It is still controversial whether the apicoplast has originated from a green or red alga during secondary endosymbiosis (Cai 2003, Funes *et al.* 2002, Kohler *et al.* 1997) but research of recent date supports red algal ancestry of the apicomplexan plastid (Coppin *et al.* 2005, Funes *et al.* 2004, Gould *et al.* 2008, Harper and Keeling 2003, Moore *et al.* 2008). The storage polysaccharide amylopectin accumulated in the cytoplasm of *T. gondii* and the dinoflagellate *Crypthecodinium cohnii* is believed to be similar to the starch accumulated by red algae. There is evidence that this storage polysaccharide is synthesized through a UDP-glucose-based pathway much simpler than that described for plants. This pathway is very similar to the one found to be encoded in the recently sequenced genome of the red algae *Cyanidioschyzon merolae* and it is distinct from the plant starch pathway (Coppin *et al.* 2005).

The apicoplast is essential to the parasites (Fichera and Roos 1997, Sullivan *et al.* 2000) as inhibition of its function or loss of the organelle leads to immediate or delayed death due to failure during invasion of new host cells (He *et al.* 2001, McFadden and Roos 1999). Apicoplast-deficient parasites replicate normally in the first infectious cycle but die in the subsequent host cell, validating the apicoplast as essential for parasite viability (He *et al.* 2001). This delayed death effect has led to speculations that the apicoplast may be required for the establishment of a functional parasitophorous vacuole. The parasitophorous vacuole is a specialized structure inside infected cells where the parasites replicate until host cell lysis (Lingelbach and Joiner 1998, Suss-Toby *et al.* 1996).

Identifying the secondary plastid in apicomplexan parasites have profound implications for development of new treatments because it represents an opportunity to target the parasites with treatments that are relatively harmless to the mammalian hosts. Recent studies of the apicomplexan genomes and protein localization together with inhibitor studies have provided some insight into the metabolism of the apicoplast. The apicoplast has a typical bacterial housekeeping machinery such as DNA replication, transcription, translation as well as anabolic pathways for synthesis of fatty acids (Waller *et al.* 1998), isoprenoid precursors (Jomaa *et al.* 1999) and some of the reactions for heme synthesis (Sato *et al.* 2004). The bacterial nature of the plastidic pathways makes them interesting as potential drug targets because they are fundamentally different from the equivalent eukaryotic pathways in their animal hosts (McFadden and Roos 1999, Ralph *et al.* 2001).

Enzymes involved in fatty acid synthesis have been localized to the apicoplast (Waller *et al.* 1998), and in *Toxoplasma* and *Plasmodium* the fatty acid biosynthesis system appears to be essential for parasite survival and virulence (Mazumdar and Striepen 2007, Mazumdar *et al*. 2006). Fatty acid biosynthesis is defined as the metabolic process by which acetyl coenzyme A (acetyl-CoA) precursors are converted to long fatty acid chains (Goodman *et al*. 2007). Fatty acids play a critical role in cells as metabolic precursors for biological membranes and energy stores (Waller and McFadden 2005). The apicoplast has a prokaryotic type II fatty acid synthesis (FAS II) that differs in structure, kinetics and inhibitor susceptibility from the eukaryotic type I fatty acid synthesis (FAS I) found in the animal hosts (Surolia *et al.* 2004, Waller *et al.* 1998). The presence of a type II pathway for fatty acid biosynthesis in the apicoplast represents a potential target for parasite-specific inhibitors (Waller *et al.* 2003).

Isoprenoid synthesis is another pathway localized to the apicoplast. The enzymes mediating the isoprenoid pathway in apicomplexan parasites are distinct from those found in the human hosts (Jomaa *et al.* 1999). The common precursor for all isoprenoids, isopentenyl diphosphate, can be produced by two different biosynthetic routes, either via the mevalonate (MVA) pathway, or via the 1-deoxy-D-xylulose 5- phosphate (DOXP) pathway. The DOXP pathway is absent in mammals, but is used by most eubacteria as well as by the plastids of algae and higher plants. In plants both pathways are present, with the DOXP pathway being operative in the plastids and the MVA pathway in the cytosol. In green algae the cytosolic MVA pathway is missing and isoprenoid supply exclusively depends on the plastidic DOXP pathway (Disch *et al.* 1998). In *P. falciparum* the biosynthesis of isoprenoids is achieved by the DOXP pathway. The enzymes of the DOXP pathway are localized inside the apicoplast and all the enzymes involved in the pathway represent potential new drug targets (Jomaa *et al.* 1999, Wiesner and Jomaa 2007). The isoprenoid synthesis in the apicoplast is the only source of isoprenes in the parasite, and it is considered to serve both the apicoplast and the mitochondrion with isoprenes (Ralph *et al.* 2004).

Genomic analysis revealed an apicoplast pathway for synthesis of heme in *P. falciparum* and *T. gondii*. In plants, the tetrapyrrole biosynthesis pathway branches and produces both heme and chlorophyll. In *Plasmodium*, the pathway seems to be split between the apicoplast, mitochondrion and possibly the cytosol. The first part of the pathway takes place in the mitochondrion and continues in the apicoplast. The following steps seem to be either mitochondrial or cytosolic, and the pathway probably terminates in the mitochondrion (Ralph *et al.* 2004).

1.3 Plastidic phosphate translocators in plants

Many of the metabolic pathways establish in plastids depend on precursors from the cytosol as well as the cytosolic pathways often require products from the chloroplast. All plastids are surrounded by envelope membranes that restrict the nonspecific diffusion of polar molecules. In plants four subfamilies of plastidic phosphate translocators (pPTs) that differ in function and substrate affinity have been identified in the inner envelope membrane of the chloroplast, the TPTs, PPTs, GPTs and XPTs (Figure 2). The transporters function as antiport systems where transport in one direction depends on simultaneous transport of another solute in the opposite direction (Flügge 1999). The TPT is involved in export of carbon from plastids, while the other transporters are importing metabolites into plastids in form of phosphoenolpyruvate (PEP), glucose-6-phosphate (Glc6P) and xylulose-5-phosphate (Xyl5P) (Eicks *et al.* 2002, Fischer *et al.* 1997, Kammerer *et al.* 1998).

The triose phosphate/ phosphate translocator (TPT) mediates export of fixed carbon from the Calvin Cycle in the form of triose phosphates and 3-PGA from the chloroplast into the cytosol for use in the biosynthesis of sucrose and amino acids. Phosphate released from these processes is transported back into the chloroplasts for production of ATP needed in the Calvin Cycle and for photosynthetic electron transport (Flügge *et al.* 1989). In C_4 -plants phosphoenolpyruvate (PEP) is exported from the chloroplast through a phosphoenolpyruvate/ phosphate translocator (PPT) and is used as substrate for the PEP carboxylase in the cytosol to form the four-carbon compound oxaloacetate. Phosphate produced in this reaction is transported back into the chloroplast. The function of PPTs in C_3-plants and nongreen tissues of C_4-plants is to import PEP from the cytosol into the plastid for use in the shikimate pathway where amino acids and secondary plant products are synthesized. Non-green plastids are not able to convert 3-PGA into PEP therefore 3-PGA produced from triose phosphates is exported from the plastid, converted into PEP in the cytosol, and then re-imported (Fischer *et al.* 1997). Cytosolically generated hexose phosphates derived from sucrose are transported by a glucose 6-phosphate translocator (GPT) into the plastids of non-green tissues as a source of carbon for starch and fatty acid biosynthesis, additionally acting as substrate for the oxidative pentose phosphate pathway (OPPP) where it is transformed into triose phosphates. Both triose phosphates and inorganic phosphate released from the starch biosynthesis can be used as counter substrates for the GPT antiporter (Kammerer *et al.* 1998). The main function of the xylulose-5-phosphate translocator (XPT) is the import of xylulose-5-phosphate (Xul-5-P)

produced in the cytosol into plastids to provide the Calvin cycle and the OPPP with carbon. The XPT subfamily is found only in dicotyledonous plants (Eicks *et al.* 2002).

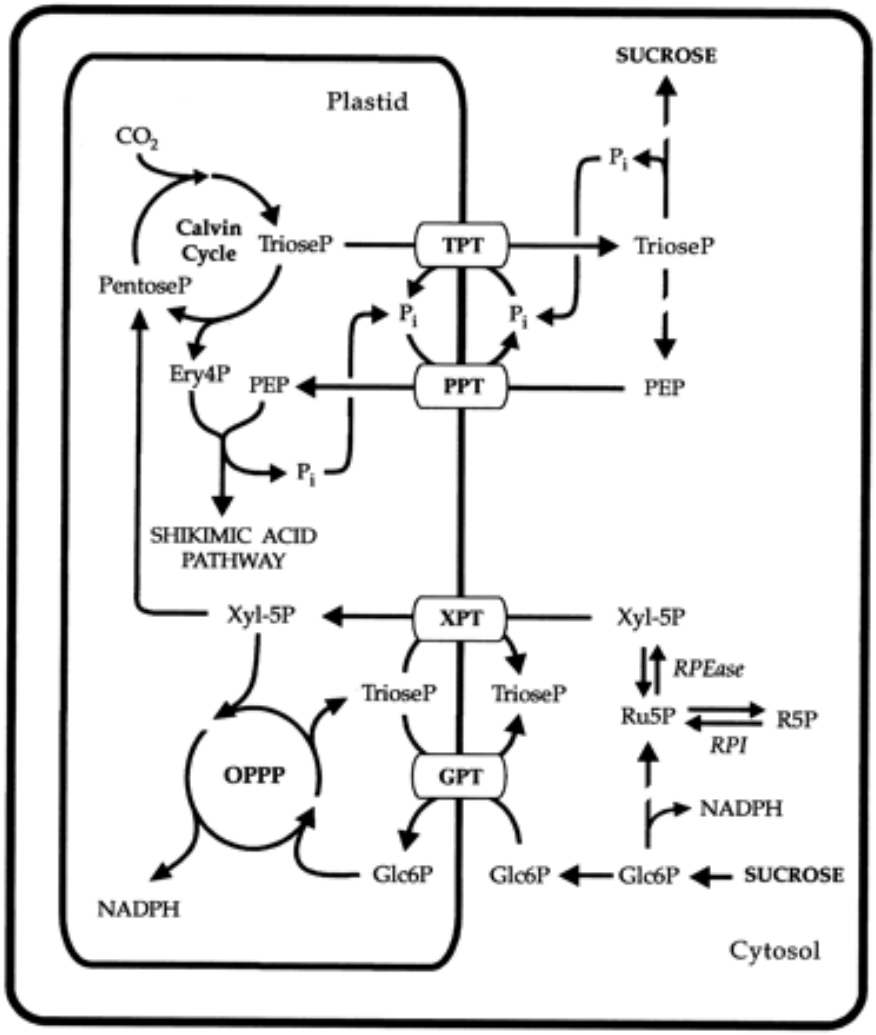

Figure 2: The proposed functions of the four plastidic phosphate translocator proteins in plants (TPTs, PPTs, GPTs and XPTs). The TPT mediates export of carbon from the Calvin cycle in the form of triose phosphates that can be converted to PEP in the cytosol. PEP is imported into the plastids via the PPT to provide the substrate for the shikimic acid pathway. The GPT imports Glc-6-P into the plastids for the syntheses of starch and fatty acids (not shown) and as a substrate for the OPPP. Triose phosphates can serve as a counter-substrate of either the GPT or the XPT. The XPT provides the plastids with Xul-5-P, which is produced in the cytosol to provide the Calvin cycle and the OPPP with carbon (Eicks *et al.* 2002).

1.4 Apicoplast phosphate translocators

Not all plastids perform photosynthesis and the lack of photosynthetic activity is compensated by feeding metabolites from the cytoplasm into the non-photosynthetic plastids (Fischer and Weber 2002). The biosynthetic pathways taking place in the apicoplast require mechanisms to provide the plastid with carbon sources, ATP and reduction power. In order to search for membrane transporters in the apicomplexan parasites the genome of *P. falciparum* was queried using chloroplast pPT protein sequences. Two highly scoring predicted proteins were identified and tested against the GenBank non-redundant database for similarity to non-apicomplexan sequences. The first protein (PfAPT1) had highest homology to a chloroplast triose phosphate translocator, the second (PfAPT2) had highest homology to the phosphoenolpyruvate translocator of chloroplasts. The same working group subsequently identified a *T. gondii* orthologue of PfAPT1, but no *T. gondii* sequence orthologous to PfAPT2 has been found to date, using plant and apicomplexan pPTs as queries of the protein and nucleotide databases (Karnataki *et al.* 2007). Given that *T. gondii* possesses only a single pPT this protein possibly is transporting more than one substrate (Fleige *et al.* 2007). The pPT in *T. gondii* is localized to the envelope membranes in the apicoplast and hence is dubbed TgPT (*T. gondii* phosphate translocator). Within the subfamilies, the plant pPTs show > 80 % identity, while across subfamilies they show about 35 % identity. The apicomplexan pPTs show a maximum of 32 % identity to the chloroplast pPTs and because specific amino acids have not been identified that definitively correlate with substrate specificity, it is not possible to assign specificity of the apicomplexan pPTs on the basis of sequence homology alone.

1.5 Aim of study

T. gondii possesses a single plastidic membrane transporter (TgPT) that shows similarity to the phosphate translocators (pPTs) in higher plants. Higher plants possess up to four pPT subfamilies with different substrate specificities (Knappe *et al.* 2003). Given that *T. gondii* possesses only one plastidic transporter it was proposed that the TgPT possibly was transporting more than one substrate (Fleige *et al.* 2007). Analyses of the apicomplexan genomes and protein localization have provided first insights into the metabolism of the apicoplast (Fleige *et al.* 2007, Jomaa *et al.* 1999, Ralph *et al.* 2004). It has been established that the apicoplast is involved in the synthesis of fatty acids (Waller *et al.* 1998), isopentenyl diphosphate (Jomaa *et al.* 1999) and heme (Sato *et al.* 2004). The proposed function of the TgPT has been to comprise a connection between the metabolic pathways in the apicoplast and the metabolic processes in the cytosol (Fleige *et al.* 2007, Roos 2002).

The apicoplast is known to be indispensable to the apicomplexan parasites, and due to its prokaryotic origin the plastid represents an attractive target for the development of parasite-specific drugs. By determining the substrate specificities of the TgPT its physiological function will be revealed and thereby give more insight into the metabolism of apicomplexan parasites. This knowledge can possibly contribute to identification of new drug targets and treatments against the parasitic diseases.

The substrate specificities of the TgPT could not be deduced from the amino acid sequence because it does not show sufficient similarity to any of the four subfamilies of higher plant pPTs. In this thesis the work has been focused at determining the substrate specificities of the plastidic phosphate translocator identified in *T. gondii.* To do so transport experiments with different phosphorylated metabolites were performed by heterologous expression of the TgPT gene in yeast and reconstitution of its transport activity in liposomes. The substrate specificities were corroborated by measurements of apparent kinetic constants for the accepted substrates, and compared with substrate specificities of phosphate translocators in higher plants and red algae.

2. Materials and Methods

In order to determine the substrate specificities of the *T.gondii* phosphate translocator (TgPT), the corresponding cDNA were cloned into BamHI/ EcoRI and HindIII/BamHI restriction sites in the yeast (*Saccharomyces cerevisiae*) expression vectors pYES-N and pYES-C (Invitrogen, see appendix) thereby adding a 6x His-tag to the N- and C-terminus of TgPT, respectively.

2.1 Electroporation

Electroporation is a mechanical method used to introduce polar molecules into a host cell through the cell membrane by electric pulses. A high-voltage electric field is applied to the cells, producing transient holes in the cell membrane through which plasmid DNA enters (Calvin and Hanawalt 1988).

LB medium, pH 7

1.0 % Tryptone

0.5 % Yeast extract

1.0 % NaCl

100 µg/ml ampicillin

Electrocompetent *Escherichia coli* (*E.coli*) cells (50 µl) were thawed on ice and incubated with 2 µl of either pYES-TgPT-N or pYES-TgPT-C for 1 min. The bacterial solution was transferred to a sterile 2 mm electroporation cuvette that was mounted into the Pulse controller (*GenePulser*, Bio-Rad) between the anode and cathode. The electroporation apparatus was set to 2.5 kV (12.5 kV/cm), 25 µF, and the pulse controller to 200 ohm. The pulse was delivered by pushing in both charging buttons simultaneously and holding until a short beep was heard. The cuvette was removed and 200 µl S.O.C medium (Invitrogen) was added immediately. The cells were transferred into a 1.5 ml tube and incubated at 37 °C for 1 h at 200 rpm. Different dilutions of the cells were spread onto selective ampicillin plates and grown overnight. Successfully transformed cells were picked and transferred to 3 ml LB-ampicillin medium for overnight growth at 37 °C.

2.2 Plasmid isolation

The *Birnboim-Doly* method for rapid extraction of plasmid DNA from *E. coli* is based on selective alkaline denaturation of high molecular weight chromosomal DNA while covalently closed circular DNA remains double-stranded. *E.coli* cells containing the plasmid of interest are lysed with sodium dodecyl sulfate (SDS) and NaOH. Denatured chromosomal DNA renature and aggregate into an insoluble precipitation when neutralized by acidic sodium acetate. The high concentration of sodium acetate also causes precipitation of protein-SDS complexes and high molecular weight RNA. The three major contaminating macro-molecules can be removed by centrifugation after precipitation with sodium acetate. The plasmid DNA is recovered from the supernatant by isopropanol precipitation (Birnboim and Doly 1979).

Solution I

50 mM Glucose

25 mM Tris, pH 8

10 mM EDTA, pH 8

Solution II

0.2 M NaOH

1 % (w/v) SDS

High salt solution

3 M Sodium acetate, pH 4.8

From an overnight culture of *E.coli,* 1.5 ml was centrifuged at 11000 x g for 1.5 min at room temperature. The supernatant was removed and the pellet was thoroughly resuspended in 100 µl of Solution I. After 5 min incubation on ice 200 µl of Solution II was added and mixed by gently pipetting three times up and down. The mixture was for a second time incubated on ice for 5 min. A volume of 150 µl ice-cold High salt solution was added and the tube vortexed immediately. The solution was centrifuged at 16000 x g for 10 min and the supernatant transferred to a new tube where it was mixed with 350 µl of isopropanol. It was again centrifuged at 16000 x g for 10 min. The supernatant was discarded and the pellet washed with 500 µl 70 % ethanol (-20 °C). It was repelleted at 16000 rpm for 5 min and dried before resuspended in 20 µl RNase-A (1 mg/ml) and incubated at 37 °C for 30 min. Plasmids were

stored at -20 °C until use. The plasmid DNA concentrations after isolation were estimated by agarose gel electrophoresis with a molecular mass ruler (MassRuler™, Fermentas).

2.3 Introduction of DNA into yeast cells

E.coli is commonly used as a host for the expression of foreign proteins, but because of the toxicity of the gene product it failed to express the plastidic phosphate translocator proteins from higher plants. Yeast has therefore previously been used for the expression of functional plastidic translocators (Flügge 1999). The uracil-auxotrophic yeast strain INVSc1 (Invitrogen) was transformed with the plasmids pYES-TgPT-N and pYES-TgPT-C by lithium acetate mediated transformation. The alkali cations from lithium acetate make intact yeast cells competent to take up DNA by addition of polyethylene glycol (PEG) followed by a heat shock (Ito et al. 1983). Successfully transformed cells were grown on selective plates.

YPD medium

1 % yeast extract

2 % peptone

2 % dextrose

10x TE-buffer

100 mM Tris, pH 7.5

10 mM EDTA

10x Lithium acetate

1 M Lithium acetate, pH 7.5

PEG 4000 solution

50 % PEG

SC-medium, 1 liter (20 g agar/ liter)

6.7 g SC-medium (Bacto-yeast nitrogen base w/o amino acids)

100 ml Drop out medium (see “yeast growth”)

2 % glucose

5 ml of YPD medium was inoculated with a single yeast colony and grown over night at 30 °C. From the saturated culture 1 µl was transferred to 300 ml of YPD medium and grown overnight at 30 °C. Cells were harvested by centrifuging 5 min at 4000 x g in room temperature. The pellet was resuspended in 10 ml of sterile water and transferred to a 15 ml Falcon tube and repelleted for 5 min at 5000 x g in room temperature. The yeast cells were resuspended in 1.5 ml freshly prepared buffered lithium solution (1 volume 10x TE buffer, 1 volume 10x lithium acetate, 8 volumes sterile water). For each transformation 200 µg carrier DNA (Single-stranded salmon sperm, Sigma) was mixed with ≤ 5 µg transforming DNA and 200 µl yeast suspension in an eppendorf tube. 1.2 ml freshly prepared PEG solution (8 volumes 50 % PEG, 1 volume 10x TE buffer, 1 volume 10x lithium acetate) was added and then incubated for 30 min at 30 °C. A heat shock was performed for exactly 15 min in a 42 °C water bath and cells pelleted by 5 seconds centrifugation in room temperature. The cells were resuspended in 500 µl 1x TE buffer and different dilutions were spread onto plates lacking uracil for selective growth of cells containing the plasmid. Incubation was performed at 30 °C until appearance of transformants (2-4 days). Successfully transformed colonies were inoculated in 5 ml cultures of selective medium lacking uracil and grown overnight at 200 rpm in 30 °C.

2.4 Plasmid DNA isolation from yeast

A rapid method for plasmid DNA isolation from yeast cells is based on breakage of the cells by vortexing with glass beads in a detergent solution, followed by a separation of nucleic acids from proteins by phenol/chloroform extraction (Hoffman and Winston 1987).

Breaking buffer

2 % Triton X-100

1 % SDS

100 mM NaCl

10 mM Tris-HCl, pH 8

1 mM EDTA, pH 8

Phenol/chloroform/isoamyl alcohol

25:24:1 (v/v/v) phenol/chloroform/isoamyl alcohol

TE-buffer

10 mM Tris, pH 7.6

1 mM EDTA

Overnight yeast cultures were harvested by centrifuging for 5 min at 1500 x g in room temperature. The cell pellet was resuspended in 200 µl breaking buffer and transferred to an eppendorf tube containing 0.3 g glass beads and 200 µl phenol/chloroform/isoamyl alcohol. The cells were broken by vortexing for 3 min at highest speed. A volume of 200 µl TE-buffer was added and vortexed briefly before centrifuged 5 min at high speed, room temperature. The aqueous layer (max 400 µl) was transferred to a clean tube which was filled up with 100 % ethanol and mixed by inversion. The tube was centrifuged again for 10 min at high speed and the pellet was washed twice with 80 % ethanol. After drying the DNA pellet was resuspended in 250 µl TE-buffer and stored at -20 °C until use.

2.5 DNA Restriction enzyme digestion

After plasmid isolation from *E.coli* the presence of a correct insert with the expected size 1031 bp, was verified by restriction enzyme digestion. Restriction enzymes or restriction endonucleases are enzymes isolated from bacteria that recognize and cut specific sequences in DNA to produce fragments, called restriction fragments. The DNA sample is first digested with restriction enzymes to generate DNA fragments, and then the different sized fragments are separated by agarose gel electrophoresis. Plasmids with correct restriction sites will generate two visible bands of DNA on the gel, and those with altered restriction sites will not be cut and will generate only a single band (Reece 2004).

In this study, plasmid DNA purified from *E.coli* by Birnboim-Doly plasmid isolation was digested to confirm whether the cloning of TgPT into the pYES-N/C vectors had been successful.

Table 1: Restriction enzymes and buffers used for N-terminal and C-terminal constructs

Construct	Restriction enzymes	Restriction buffer
N-terminal	EcoRI / BamHI	EcoRI buffer
C-terminal	HindIII / BamHI	HindIII buffer

Table 2: Mastermix for restriction enzyme digestion

Reagent	Volume
Restriction enzymes	0.5 µl of each
Restriction buffer	1 µl
DNA*	2 µl
dH_2O	6 µl

*****Plasmid DNA isolated from *E.coli*

For each reaction, 2 µl plasmid DNA was added to 8 µl of mastermix. The digestion was carried out for 2 hours at 37°C. The restriction fragments were separated by 1 % agarose gel electrophoresis and visualized by ethidium bromide staining.

2.6 Polymerase Chain Reaction

Polymerase Chain Reaction (PCR) is a method for enzymatic amplification of specific sequences of DNA. Knowledge of the DNA sequence flanking the sequence of interest is required in order to produce synthetic complementary primers that are needed to initiate the amplification process. The PCR reaction goes through three different steps defined by the critical aspects of time and temperature; denaturation, annealing and elongation, these steps make up a cycle that is repeated 20-35 times to achieve a satisfying amount of amplified DNA In the denaturation step, the PCR reaction is heated to a temperature of around 95 °C where the hydrogen bonds of the double helix are broken resulting in single-stranded molecules to be used as templates. In the annealing step, the reaction temperature is lowered to around 50-60°C so that the primers can anneal to the single-stranded DNA template forming short segments of double-stranded DNA where the polymerase attaches and begins DNA synthesis. During the extension/elongation step, the DNA polymerase synthesizes new DNA strands complementary to the DNA template strands (Reece 2004, Wilson and Walker 2000).

To verify correct insertion of the construct into the yeast strain InvSc1 after lithium acetate mediated transformation, plasmid DNA was isolated from the yeast cells by phenol/chloroform mediated DNA isolation and used as template for PCR reaction. The TgPT gene was amplified using the primers Toxo1 (5`-ACTTCTTCGTCCACATCGGC) and Toxo2 (5`-TTTCGCGATGATCTGCTGGC) (Sigma).

Table 3: Standard PCR Mastermix

Reagents	**Volume**
10X buffer	5 µl
Forward primer	1µl
Reverse primer	1 µl
dNTP	1 µl
Taq Polymerase	0,6 µl
dH_2O	40,5 µl

Table 4: PCR program. * Repeated 35 cycles

Phase	Time	Temperature
Initial denature	2 min	95 °C
Denature*	30 sec	94 °C
Anneal*	15 sec	55 °C
Elongation*	1 min	72 °C
	10 min	72 °C
Cooling	∞	4 °C

The PCR reactions were performed with a DNA EngineGradient Cycler PTC-200 (MJ Research)

Mastermix (49 µl) and plasmid DNA (1 µl) were mixed in a PCR tube to a total volume of 50 µl. The PCR thermo cycler was programmed according to table 4. The program start with a 2 minutes denaturation at 95 °C, and after 35 cycles the program end with a 10 minutes elongation followed by a 4 °C unlimited hold. The PCR products were separated by agarose gel electrophoresis and detected by ethidium bromide staining.

2.7 Agarose gel electrophoresis

Agarose gel electrophoresis is a method used to separate nucleic acids; DNA or RNA molecules by size. This is achieved by moving negatively charged nucleic acid molecules through an agarose matrix with an electric field (electrophoresis). The negative charge of the molecules is due to the phosphate backbone they possess. Shorter molecules move faster and migrate farther than longer ones and by varying the concentration of agarose, one can separate varying ranges of DNA fragment sizes (Sambrook 2001). The separated DNA fragments are stained with ethidium bromide for visualization on the gel by UV-light. The binding of ethidium bromide to DNA results in distortion of the double helix and increases its overall length. DNA to which ethidium bromide is bound fluoresces under UV-light. The size of the DNA fragments can be determined by comparing them to DNA-ladders with fragments of known size (Reece 2004).

1% Agarose gel

0.6 g agarose

60 ml TBE buffer

1 µl ethidium bromide (5 µg/ml)

TBE-buffer

89 mM Tris, pH 7.6

89 mM boric acid,

2 mM EDTA

To make a 1 % gel, 0.6 g agarose was boiled in 60 ml TBE-buffer to dissolve. The liquid agarose was mixed with 1 µl ethidium bromide, poured into a casting frame with a comb to make the wells and left to polymerize for 30 min. The gel was then placed in an electrophoresis tank containing TBE-buffer as the running buffer. Loading buffer (6 x DNA Loading Dye, Fermentas) was added to the samples before loaded into the wells. In this study, GeneRuler™ 1 kb DNA Ladder and GeneRuler™ DNA Ladders Mix (Fermentas) were used as size markers. The gel was run for 60 min at 90 volts and DNA bands visualized by UV light using a Gel Doc 2000 (BioRad).

2.8 Yeast growth

The yeast strain *Saccharomyces cerevisiae* has several properties which have established it as an important tool in the expression of foreign proteins for research, industrial or medical use. Yeast can be grown rapidly on simple media to high cell density and its genetics are more advanced than any other eukaryote (Romanos *et al.* 1992). The gene encoding the TgPT protein is under control of a galactose regulated promoter which is controlled by two regulatory proteins and the carbon source in the medium. When galactose is present, the two regulatory proteins interact and activate transcription. In the absence of galactose the transcriptional activation is blocked, and in the presence of glucose the transcription of the galactose genes are strongly repressed (Johnston et al. 1994).

SC-medium, 1 liter

6.7 g SC-medium (Bacto-yeast nitrogen base w/o amino acids)

100 ml Drop out medium

50 ml glucose/galactose (40%) Fill up with dH_2O

10X Drop out (DO) medium for yeast culture, 1 liter

Isoleucine	300 mg	
Valin	1500 mg	
Adenine	200 mg	
Arginine	200 mg	
Histidin	200 mg	
Leucine	1000 mg	
Lysine	300 mg	
Methionine	200 mg	
Phenylalanine	500 mg	
Threonin	2000 mg	
Tryptophan	200 mg	Fill up with dH_2O

Single colonies of yeast were inoculated into 5 ml of SC-medium containing 2 % glucose and grown over night at 30°C with shaking at 200 rpm. The overnight culture was transferred into a 50 ml culture and grown over night at 30°C with shaking at 200 rpm. The cells were centrifuged at 1500 x g for 5 min at 4°C and the supernatant discarded. Then the cells were

resuspended in 2 x 400 ml SC-medium containing 2 % galactose to induce the expression of mTgPT-N and mTgPT-C, and grown at 30 °C with shaking at 200 rpm. After 8 hours the induction was terminated by harvesting the cells with centrifugation at 1500 * g for 5 min. The cells were stored at -20°C until ready to use (Protocol from Invitrogen Catalogue nos. 8252-20).

2.9 Membrane preparation

Exogenous proteins in yeast are targeted to membrane-bound compartments that are readily isolated for biochemical experiments (Ton and Rao 2004).

1X TE-buffer

10 mM Tris/HCl, pH 7.5

1 mM EDTA

PMSF

100 mM in EtOH

Glass beads (~ 0.5 mm)

Glass beads were incubated with 0.1 M HCl overnight. Then they were washed under running water for an hour, before adding sterile water and checking the pH. The glass beads were dried over night using filter paper.

All steps were conducted at 4 °C using precooled media and equipment. After thawing, the yeast cells were disrupted in 210 µl TE-buffer containing 100 mM protease inhibitor Phenyl-methyl-sulfonyl-fluoride (PMSF). The cells were transferred to 1.5 ml eppendorf tubes containing 400 mg glass beads for homogenization by strong shaking in 6 min at 4°C (TissueLyser II, Qiagen). The cell remains were separated from the membranes by adding 750 µl TE/PMSF and shaking by hand before centrifuging in 45" at 1000 rpm. This was repeated by transferring the supernatant to new tubes and centrifuging in 45" at 1000 rpm. The supernatant was transferred to new tubes with part of the lid cut off and centrifuged for 25 min at 45000 rpm (Optima™ L-100 XP Ultracentrifuge). The pellets were frozen in liquid nitrogen and stored at – 80 °C until use. The protein concentrations were measured by Bio-Rad (Bradford) Protein Assay, a dye-binding analysis in which a differential color change of a dye occurs in response to various concentrations of protein.

2.10 Purification of Phosphatidylcholine

Phosphatidylcholine (100 g) was dissolved in 320 ml chloroform and separated by adding 1.4 liter of ice-cold acetone by continuous stirring for 1 hour. The lipids were precipitated over night at 4°C. The precipitate was dissolved in 320 ml diethyl ether and extracted under vacuum in a rotting flask. When the ether was completely evaporated the purified lipids were stored at -20 °C until use.

2.11 Preparation of liposomes

Liposomes are artificially constructed vesicles of a lipid bilayer enclosing an aqueous compartment (Szoka and Papahadjopoulos 1980). The system allows accurate measurement of solute transport from one compartment to another by reconstituted membrane proteins (Hanke et al. 1999). The TgPT transport activity was reconstituted into preloaded liposomes in order to determine the substrate specificities.

Liposome buffer (preloaded liposomes)

100 mM Tricin/KOH, pH 7.6

30 mM K-gluconate

20 mM substrate (P_i, 3-PGA, PEP, TP or Glc6P)

Liposome buffer (empty liposomes)

100 mM Tricin/KOH, pH 7.6

60 mM K-gluconate

PD-10 buffer

100 mM Na-gluconate

50 mM K-gluconate

10 mM Tricin/KOH, pH 7.6

The liposomes were preloaded with exchangeable substrates by adding liposome buffer (1 ml/ kinetic) containing a phosphorylated metabolite to the purified phospholipids (125 mg phospholipids/ 1 ml liposome buffer). By sonication for some minutes on ice (duty cycle: 20%, output: 5) the lipids were broken into liposomes. The membrane pellets isolated from yeast cells were dissolved in 100 µl dH_2O and the proteins were solubilized from the

membranes by adding 7 µl 20 % Triton X-100. The protein solution was added to the liposomes (50 µl membranes/ 750 µl liposomes), mixed by inversion and frozen in liquid nitrogen. The frozen liposomes were thawed on ice and sonicated with 30 pulses (duty cycle: 30, output: 5) to integrate the proteins into the membranes (Kasahara and Hinkle 1977). PD-10 columns (Amersham Biosciences) were equilibrated by washing with 3 x 5 ml PD-10 buffer. The columns contain Sephadex™ G-25 for size exclusion chromatography that allows separation of liposomes preloaded with substrate from the external solution. For each column 900 µl of liposomes were loaded and eluted with 3 ml PD-10 buffer. When the flow-through turned white, 1 ml of liposomes was collected in an eppendorf tube.

2.12 Transport experiment

The transport activity of the TgPT protein reconstituted into liposomes is measured as movement of radiolabelled substrate into the liposomes. Radioactively labeled inorganic phosphate [^{32}P] (purchased from Amersham-Pharmacia, Germany) and cold P_i is added to the surrounding extracellular fluid and will be transported into the liposomes in exchange with preloaded substrate. The transport rate is quantified at different time points by liquid scintillation counting (Hanke *et al.* 1999).

Na-acetate buffer

150 mM Na-acetate

Substrate solution

2 µCi $^{32}PO_4$ per kinetic

10 mM KH_2PO_4

For each kinetic 850 µl of the liposome solution was mixed with 45 µl of substrate solution, and 200 µl from this was loaded on the columns at time points 15", 35", 55" and 75". To terminate the transport activity external radioactivity was removed by passing the suspension over a column preloaded with Dowex AG1-X8 resin (Bio-Rad) to bind charged particles in the extracellular fluid. The anion exchange columns were prepared from Pasteur pipettes with cotton and pre-equilibrated with 150 mM Na-acetate buffer. The liposomes were eluted with 2 x 850 µl Na-acetate buffer and collected in scintillation tubes. The radioactivity of the eluate was determined by liquid scintillation counting.

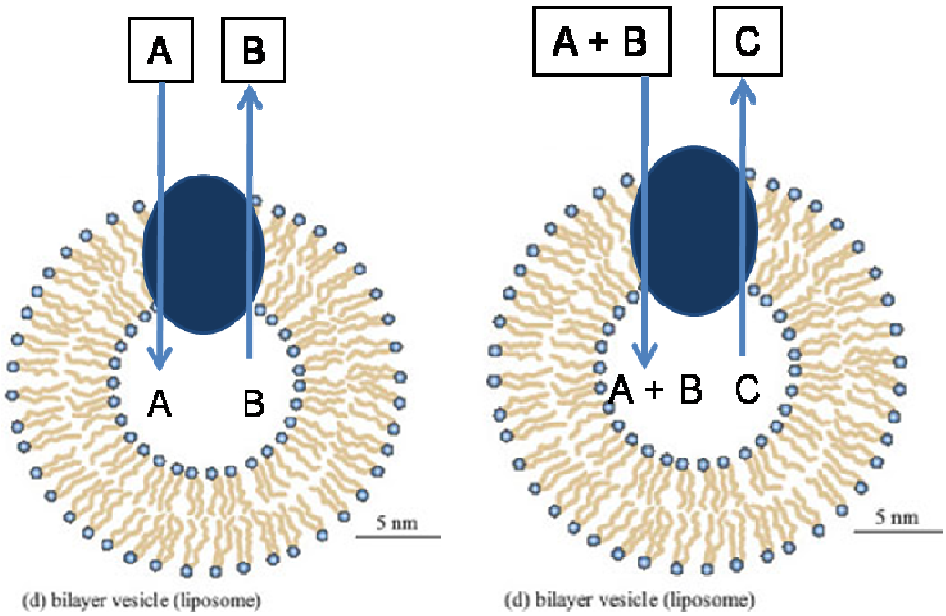

Figure 3: Experimental setup for transport measurements with the TgPT antiporter. In the first setup liposomes were preloaded with the substrate of interest and radioactively labeled phosphate [^{32}P] was used as counter exchange substrate to get an indication which metabolites the TgPT accepts as substrates. To determine the affinity to phosphate (K_m) the liposomes were preloaded with phosphate, and [^{32}P] used as counter exchange substrate. The second setup illustrates a competitive binding experiment used to determine the affinity of non-radioactively labeled substrates. The binding of [^{32}P] was measured in the presence of the unlabeled substrates. All liposomes used for the competitive binding experiment were preloaded with 20 mM inorganic phosphate. A: [^{32}P]-P_i, B: Unlabeled inhibitors (PEP, 3-PGA, TrioseP, Glc6P), C: inorganic phosphate.

2.13 SDS-PAGE

Sodium dodecyl sulfate polyacrylamide gel electrophoresis (SDS-PAGE) is a method used for separating proteins according to their electrophoretic mobility. Sodium dodecyl sulphate (SDS) is an anionic detergent which denatures secondary and non–disulfide–linked tertiary structures, and applies a negative charge to each protein in proportion to its mass. The proteins migrate in response to an electrical field through pores in the gel matrix. The combination of gel pore size and protein charge, size and shape determines the migration rate of a protein (Reece 2004).

Sample buffer

0.125 M Tris-HCl, pH 6.8

4 % (w/v) SDS

20 % (v/v) Glycerin

10 % (v/v) 2-Mercaptoethanol

0.01 % (w/v) Bromo-phenol blue

10X Laemelli buffer

250 mM Tris

1.92 M Glycine

1 % SDS

Table 5: Reagents and volumes for polyacrylamide gels

	Stacking gel, 4 %	Separation gel, 12 %
dH_2O	2,7 ml	3,4 ml
Acrylamide, 30 %	0,67 ml	4,0 ml
Tris 1,5 M/ 1 M	0,5 ml	2,5 ml
SDS, 10 %	40 µl	90 µl
APS, 10 %	25 µl	60 µl
TEMED	6 µl	40 µl

The SDS-PAGE was carried out according to the Laemelli protocol from 1970. The separating gel was prepared and allowed to polymerize on the bottom of the cast before pouring the stacking gel on top. Due to the higher acrylamide percentage in the separating gel, the proteins will be concentrated on the interface between the two gels resulting in increased protein resolution. After complete polymerization the chamber was assembled and Laemelli buffer poured into the well. Each membrane pellet were solubilized in 100 µl sample buffer and loaded onto the gel (5 – 25 µl per/lane). The electrophoresis was carried out at 80 V for 1-2 hours, using Power Pac 300 (Bio-Rad).

2.14 Silver staining

Silver staining is a sensitive tool used for protein visualization after polyacrylamide gel electrophoresis with a detection level down to 0.3-10 ng. The protein detection depends on the binding of silver ions to the amino acid side chains, followed by reduction to free metallic silver. The protein bands are visualized as spots on the gel where the reduction occurs (Switzer et al. 1979).

Fixing solution

50 % (v/v) Methanol

12 % (v/v) Acetic acid

0.019 % (v/v) Formaldehyde

Washing solution I

50 % (v/v) Ethanol

Washing solution II

615 mM Sodium Thiosulfate

Staining solution

0.2 % (w/v) Silver nitrate

0.075 % (v/v) Formaldehyde

Developing solution

0.57 M Sodium carbonate

0.019 % (v/v) Formaldehyde

17.3 µM Sodium Thiosulfate

Stop solution

50 % (v/v) Methanol

12 % (v/v) Acetic acid

After electrophoresis the gels were fixed over night to restrict protein movement from the gel matrix and to remove interfering ions and detergent from the gel. The gels were then washed in 50 % ethanol for 3 x 20 min to remove the remaining detergent ions. To increase the sensitivity and the contrast of the staining the gels were incubated for 1 min in solution III, and rinsed three times with dH_2O. The gels were then incubated in the staining solution for 20 min. When staining was complete, gels were rinsed in dH_2O and moved to developing solution. The reaction was stopped by adding stop solution when the desired intensity of the bands was reached.

2.15 Western Blot

Western blotting is a useful method for the identification and quantification of specific proteins. Proteins are usually separated using SDS-PAGE before transferred to a membrane where they are probed by antibodies specific to the target protein. Following a blocking step to prevent any nonspecific binding of antibodies to the surface of the membrane, the membrane is probed with a primary antibody that attaches to the antigen of interest. After a washing step, the membrane is incubated with a secondary antibody that is reactive toward the primary antibody. After probing with secondary antibody, the membrane is washed again and incubated with an appropriate enzyme substrate (Towbin *et al.* 1979). One of the substrates used for protein detection is luminol-based and produce a chemiluminescent signal. Chemiluminescence is a chemical reaction that produces energy released in the form of light in the presence of horseradish peroxidase and a peroxide buffer. The intensity of the signal after development should correlate with the abundance of the antigen on the membrane (http://www.piercenet.com/files/WBGuide.pdf).

In this study, protein samples after membrane preparation were resolved by SDS-PAGE before they were transferred to a Polyvinylidene Fluoride (PVDF) membrane, where they were detected by HisProbe™ (Pierce) directed against the polyhistidine tag.

Blocking buffer

4 % (w/v) Milk powder

1X TBS buffer Stored at 4° C

10X TBS buffer

100 mM Tris-HCl, pH 7.5

1.5 M NaCl

TBS-T buffer

3X TBS buffer

0.05 % (v/v) Tween 20

0.2 % (v/v) Triton X-100

10X WBB

20 mM Tris

150 mM Glycine

Cathode buffer

1X WBB

0.1 % SDS

Anode buffer

1X WBB

30 % Methanol

The blot was built from the anode side starting with two sheets of filter paper soaked in anode buffer. The transfer membrane was incubated in methanol followed by anode buffer, and placed on top of the filter paper. The gel was soaked in cathode buffer and laid on top of the membrane, and then covered by two more filter papers soaked in cathode buffer. The system was closed and current was applied for 1.5 hours, 0.65 mA / cm^2 membrane.

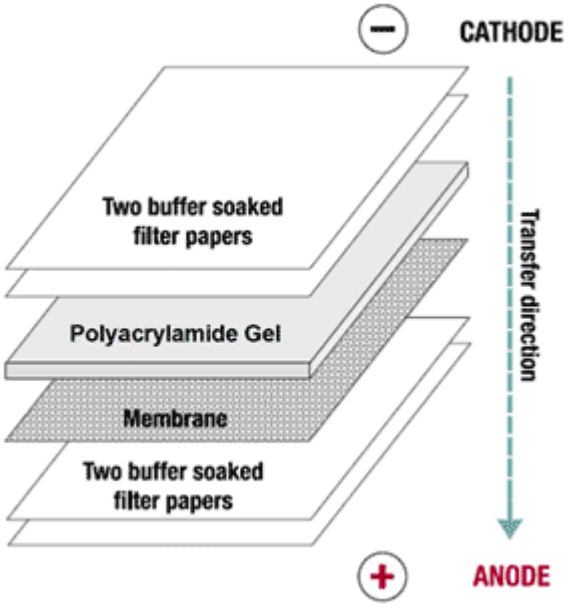

Figure 4: Schematic illustration of the western blot set up. Starting from the anode side with two sheets filter paper soaked in anode buffer, followed by membrane and gel, ending at the cathode side with two filter papers soaked in cathode buffer

After transfer the membrane was washed twice in TBS solution for 10 minutes each and incubated over night in blocking solution at 4 °C. Following, the membrane was washed 2 x 10 min in TBS-T solution before incubating for 1 hour in HisProbe™-HRP Working Solution (diluted 1:5000 in TBS-T). The membrane was washed four times in TBS-T for 10 minutes each. Equal volumes of Luminol/Enhancer Solution and Stable Peroxide Solution (SuperSignal®West Pico, Pierce) were mixed and the membrane was incubated in the solution for 5 min. The blot were removed and wrapped in transparent foil before signals were detected by a Fluor-S™ Max MultiImager (BioRad).

3. Results

In order to determine the substrate specificities of the *T.gondii* phosphate translocator (TgPT) cDNA encoding the transport protein was cloned into the yeast expression vectors p-YES-N and pYES-C (Invitrogen), resulting in the proteins mTgPT-N and mTgPT-C. After amplification in *E.coli*, the plasmids were transformed into the yeast strain INVSc1 for heterologous expression of the proteins, followed by a reconstitution of their transport activities in liposomes. Western blot analyses were performed to verify yeast expression of the TgPT after galactose mediated induction. Total membranes were isolated from yeast cells and solubilized proteins were integrated into liposome membranes. For antiport membrane proteins the transport in one direction depends on simultaneous transport of another solute in the opposite direction. Thus, the liposomes were preloaded with an exchangeable metabolite and radioactively labeled phosphate, [^{32}P]-$P_{i,}$ was used as external counter exchange substrate. The transport activity for different metabolites was measured using liquid scintillation counting of the amount [^{32}P] imported into the liposomes after a given time of transport activity.

The substrate specificities of the TgPT were corroborated by calculation of the kinetic constants for the substrates accepted by the transporter. The kinetic data from the transport experiments were analyzed according to the Michaelis-Menten model to determine apparent K_m and K_i values for the different substrates. For precise calculations of the kinetic constants the data were converted by taking the reciprocals of the Michaelis-Menten equation and graphically present the data in a Lineweaver-Burk plot. The substrate specificities of the TgPT were compared with substrate specificities of phosphate translocators in higher plants and red algae.

3.1 Amplification of cDNA in *E.coli*

The corresponding cDNA of the TgPT protein was cloned into the yeast expression vectors pYES-N and pYES-C (Invitrogen), which are 6 x His-tag fusion vectors with a galactose-inducible promoter. Electrocompetent *E.coli* cells were transformed with pYES-TgPT-N and pYES-TgPT-C to amplify the plasmids before transformation into yeast cells. Plasmid DNA was isolated from *E.coli* by the Birnboim-Doly method and the presence of correct insert TgPT gene was confirmed by restriction enzyme digestion with the restriction enzymes BamHI /EcoRI for the N-terminal fusion and HindIII / BamHI for the C-terminal fusion. The different sized restriction fragments were separated on a 1 % agarose gel and visualized by ethidium bromide staining.

The restriction fragments after digestion of the N-terminal fusion vector from three different plastid isolations are shown in figure 5. Expected band sizes were 1031 bp and 6000 bp.

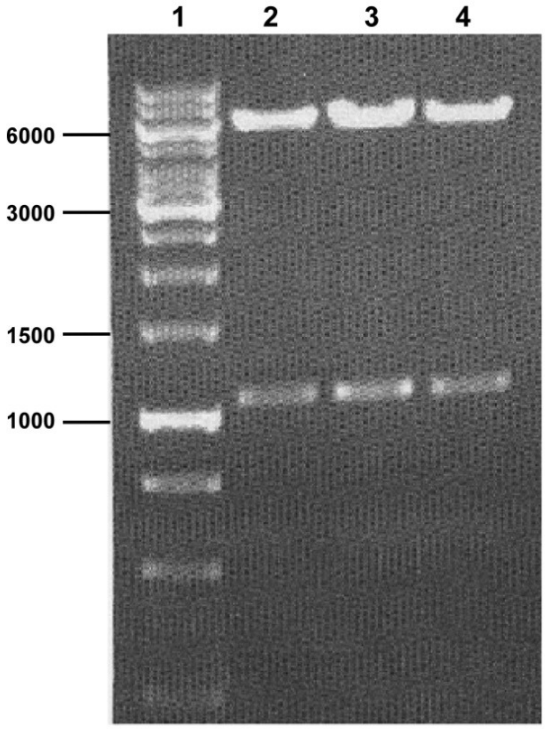

Figure 5: Gel electrophoresis showing fragments of pYES-TgPT-N isolated from *E.coli* after restriction enzyme digestion. A restriction enzyme digestion of pYES-TgPT-N was performed with the restriction enzymes BamHI and EcoRI, followed by an agarose gel electrophoresis to separate and visualize the restriction fragments. Lane 1: GeneRuler™ 1 kb DNA Ladder (Fermentas), Lane 2-4: products after restriction enzyme digestion with BamHI and EcoRI. Fragments corresponding to sizes 1031 and 6000 bp can be seen in all three lanes.

The results show that all three digestion reactions gave bands at predicted sizes, (Figure 5, lane 2-4), confirming that the cloning of TgPT into the pYES-N vector was successful. Digestion of the C-terminal fusion vector gave similar results (data not shown).

3.2 Introduction of TgPT into the yeast strain INVSc1

Plasmids containing the TgPT gene were transformed into competent cells from the uracil-auxotrophic yeast strain INVSc1 to produce protein required for the transport experiments. Yeast cells containing the plasmid after transformation were selected for on selective plates lacking uracil, and several colonies were checked for correct insert by PCR with Toxo1 and Toxo2. The primers are specific for the TgPT gene and should amplify a region of 470 bp. Untransformed yeast cells were used as negative controls.

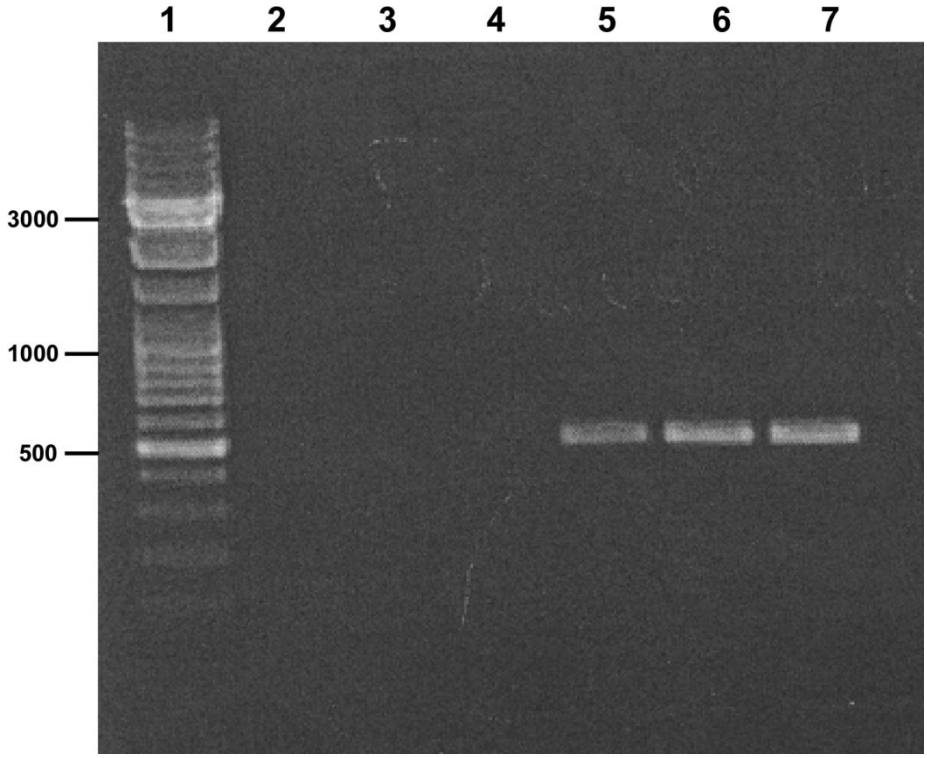

Figure 6: Gel electrophoresis showing PCR products after amplification with primers specific for the TgPT gene. Plasmid DNA from yeast cells were used as template. Lane 1: GeneRuler™ DNA Ladders Mix (Fermentas), Lane 2-4: untransformed yeast (negative control), Lane 5-7: yeast transformed with pYES-TgPT-N. Lane 5-7 show bands at the predicted size, ~470 bp, after amplification.

Results presented in figure 6 show that the yeast strain INVSc1 contains the pYES-TgPT after transformation. As expected, negative controls (Figure 6, lane 2-4) show no bands. Successfully transformed yeast cells were picked and grown in selective liquid cultures (SC-medium lacking uracil) for further use in transport experiments.

3.3 Heterologous expression of TgPT in INVSc1

In order to verify expression of the recombinant TgPT protein in the yeast transformants and to optimize the induction time, cells were grown in the presence of galactose and harvested at different time points ranging from 2 to 24 hours after induction. Membrane fractions were prepared by strong shaking with glass beads and high speed (45000 x g) centrifugation. Proteins were separated by SDS-PAGE, and western blot analysis with HisProbe™ (Pierce) directed against the polyhistidine tag verified the galactose-inducible accumulation of the TgPT protein compared to a control, which maintained the empty expression vector.

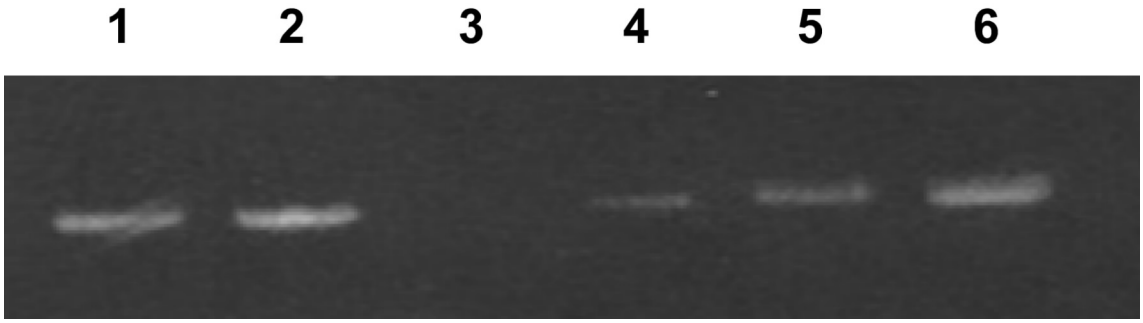

Figure 7: Western blot detection of the TgPT protein by HisProbe™ (Pierce). The results verify expression of the TgPT gene in yeast (Lane 1-2) and are showing an increasing signal with prolonged exposure to galactose (Lane 4-6). Lane 1-2: TgPT expression after 8 hours induction, Lane 3: empty vector (negative control), Lane 4: TgPT expression after 2 hours induction, Lane 5: 4 hours induction, Lane 6: 8 hours induction

The western blot verified protein expression after galactose mediated induction (Figure 7, lane 1-2). As expected, no signal was detected in the protein fraction from cells transformed with an empty vector (Figure 7, lane 3). There was an increasing expression with time between 2 and 8 hours post-induction (Figure 7, lane 4-6), but no further enhancement of expression thereafter (data not shown).

A number of transformed yeast colonies were screened by western blotting in order to identify colonies strongly expressing the TgPT. The signal intensity detected on the blot was compared with amount of protein visualized by silver staining after SDS-PAGE. A strong signal on the blot together with a corresponding weak signal on the silver stained gel indicates a high protein expression rate.

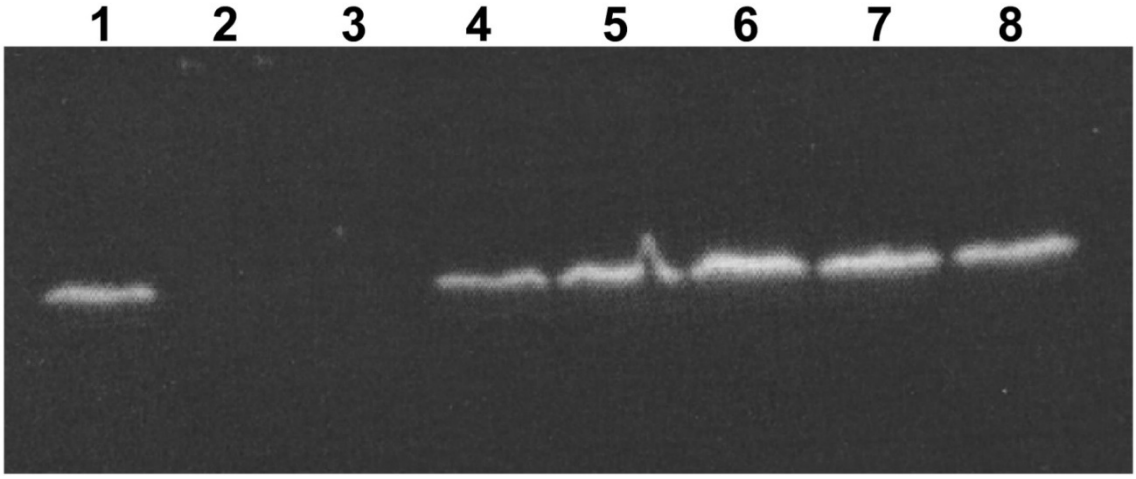

Figure 8: Western blot detection of the TgPT protein in different clones by HisProbe™ (Pierce). Show significant expression of the protein in 6 of 8 colonies. Lane 1-8: TgPT expression in different colonies after 8 hours galactose induction.

The results presented in figure 8 show similar expression levels in 6 of 8 colonies after screening. The absent signal in lane 2 and 3 indicate colonies either missing the insert or having very low expression level.

After analyzing the TgPT expression level of different clones by western blot and silver staining, one clone was chosen for further experiments. Yeast cells were grown in selective SC-medium over night and harvested after 8 hours of galactose induction. Total yeast membrane fractions were isolated and reconstituted into liposomes for transport experiments.

3.4 Determination of substrate specificities

The heterologous expression of cDNAs encoding transport proteins in yeast and the reconstitution of their transport activity in liposomes has been used as method for functional characterization for several members of the plastid phosphate translocators in plants (Eicks *et al.* 2002, Fischer *et al.* 1997, Kammerer *et al.* 1998, Loddenkotter *et al.* 1993). In order to determine the substrate specificities of the TgPT, liposomes were prepared by sonication of acetone-washed phosphatidylcholine in a buffered solution containing an exchangeable substrate for preloading. Proteins were purified from yeast membranes by using Triton X-100 as detergent and incorporated into the liposomes by a freeze/thaw step followed by sonication. The transport experiments were started by addition of [^{32}P]-P_i as the external counter exchange substrate to liposomes containing unlabeled substrate, and terminated at different time points by passing the liposomes over an anion exchange column. The activity was determined by liquid scintillation counting.

The phosphate transport activities of both the N- and C-terminal fusion proteins were determined. Yeast membrane fractions from cells transformed with an empty vector (NTC) were used as negative control to determine the background transport activity of endogenous yeast proteins. Additionally, transport with empty liposomes (EN) was performed as control to confirm that there was no substrate transport into the liposomes unrelated to the TgPT.

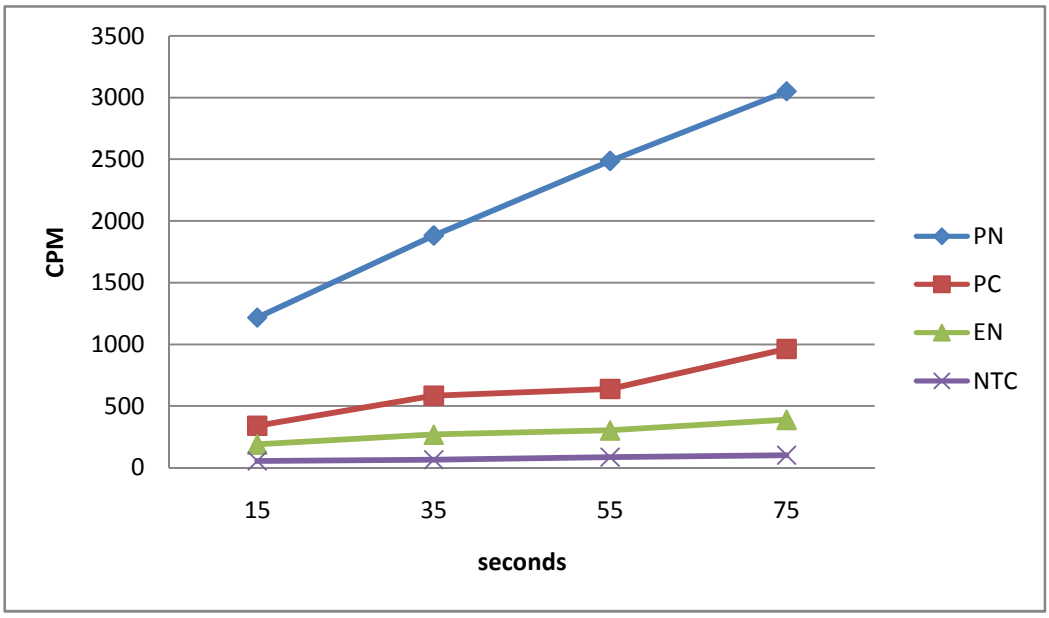

Figure 9: Determination of the phosphate/phosphate counter exchange activity. Uptake of inorganic phosphate in the presence and absence of phosphate (10 mM) preloaded to the liposomes. PN: TgPT with N-terminal fusion of His-tag, PC: TgPT with C-terminal fusion of His-tag, EN: TgPT reconstituted into empty liposomes, NTC: cells transformed with an empty vector. Counts per minute (CPM) is the number of atoms in a given quantity of radioactive material that are detected to have decayed in one minute.

The protein with C-terminal fusion (PC) showed a transport activity that makes up less than 30 % of the activity possessed by the protein with an N-terminal fusion (PN) (Figure 9). Therefore, only the N-terminal fusion protein was used for further experiments. Virtually no phosphate uptake occurred in the absence of a suitable counter substrate within the liposomes (EN), demonstrating the antiport function of the reconstituted translocator. The control transformed with an empty vector (NTC) to determine background transport activity of endogenous yeast proteins showed a negligible transport activity.

In order to determine which metabolites are accepted as substrates by the TgPT, liposomes were preloaded with different metabolites (10 mM) and [^{32}P]-P_i (10 mM) was used as external counter exchange substrate. The amount of [^{32}P] transported into the liposomes in exchange with the preloaded substrates was measured by liquid scintillation counting after different length of transport activity.

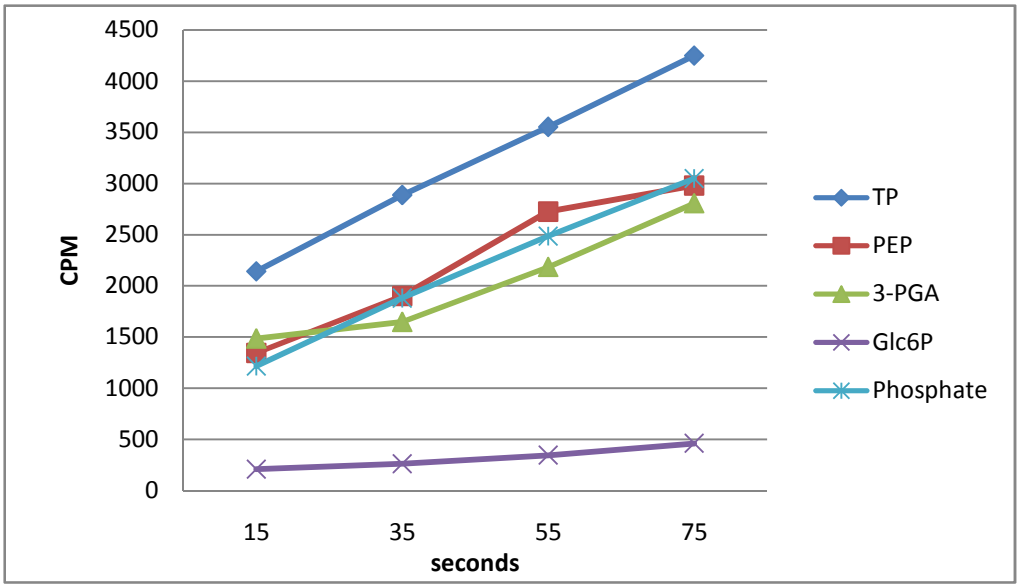

Figure 10: Determination of substrate affinities by transport experiment. Transport activities were measured for substrates transported by the TgPT reconstituted into liposomes that had been preloaded with different metabolites. The graph show amount of [^{32}P] transported into the liposomes after 15, 35, 55 and 75 seconds. TP: triose phosphate, PEP: phosphoenolpyruvate, 3-PGA: 3-phosphoglycerate, Glc6P: glucose-6-phosphate.

After initial experiments with different metabolites preloaded to the liposomes, glucose-6-phosphate (Figure 10), fructose-1-phosphate and glucose-1-phosphate (data not shown) obviously cannot be transported by the TgPT, and were not used for further transport experiments in order to determine the kinetic constants. Evidently, PEP, 3-PGA and inorganic phosphate are about equally well accepted as countersubstrates by the TgPT, while triose phosphates display an even higher transport rate.

The transport experiments carried out to determine substrate specificities was repeated in at least three independent experiments under similar conditions. The transport activity for the different metabolites was calculated as percentage of the phosphate/phosphate transport activity, which was set to 100 %, and compared with substrate specificities of pPTs from higher plants and red algae (Table 6).

Table 6: Substrate specificities of plastidic phosphate translocators from *T.gondii* (TgPT, this thesis), red algae (TPT, PPT) (Linka *et al.* 2008) and higher plants (TPT, PPT, GPT) (Kammerer *et al.* 1998). The phosphate transport proteins were isolated from yeast cells and reconstituted into liposomes that had been preloaded with the indicated substrates. Activities are given as percentage of the Pi/Pi counter exchange activity.

	TgPT	GsTPT	GsPPT	SoTPT	BoPPT	PsGPT
Phosphate	100	100	100	100	100	100
Triose phosphate	**192** ± 50	**87**	25	**92**	22	**112**
3-PGA	**167** ± 34	25	22	**90**	16	50
PEP	**99** ± 16	20	**90**	5	**72**	20
Glucose-6-P	25 ± 5	25	15	5	2	**90**

Data for TgPT are summarized as the mean ± SE of at least three independent experiments

Obviously, the TgPT protein accepts inorganic phosphate and PEP equally as substrates, having an even higher affinity to triose phosphates and 3-PGA (Table 6). The substrate specificities of pPTs from red algae (Linka *et al.* 2008) and higher plants (Kammerer *et al.* 1998) were compared with data from the phosphate translocator in *T.gondii* (Table 6). Higher plants possess up to four different pPTs with different substrate specificities (Flügge 1999), while *T.gondii* has only one pPT that obviously combine the substrate specificities of both TPTs and PPTs. Red algae on the other hand possess both TPTs and PPTs that are accepting triose phosphates and PEP, respectively. The TPT in red algae are lacking the 3-PGA transport function found in higher plants and *T. gondii* (Linka *et al.* 2008).

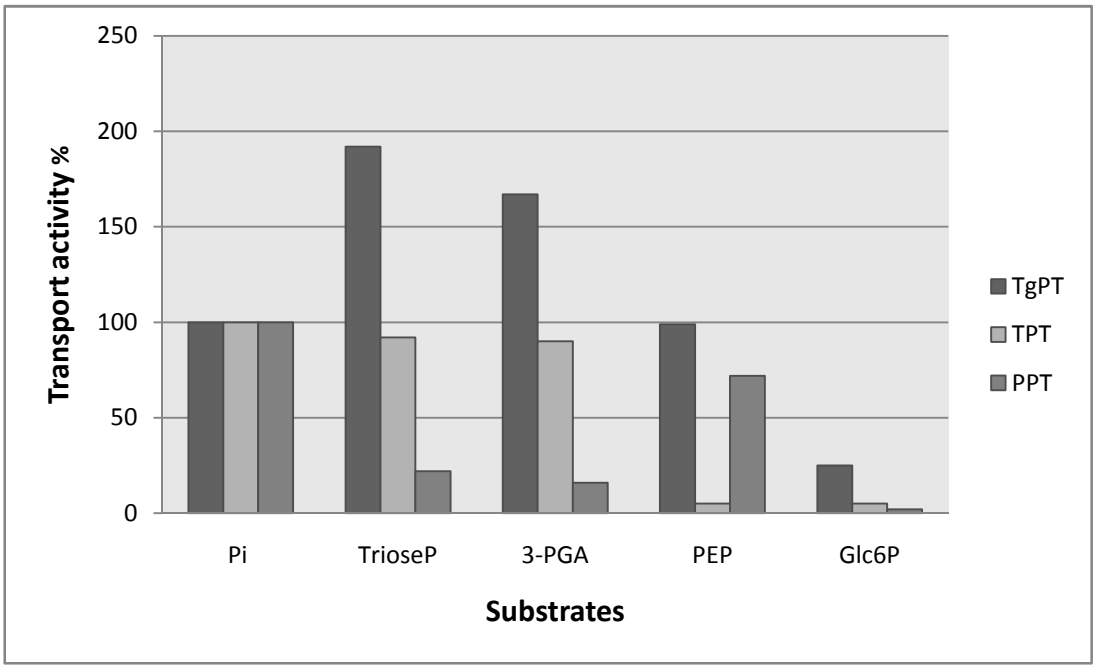

Figure 11: Substrate specificities of the TgPT, TPT and PPT. *T.gondii* have only one pPT (TgPT) that combines the substrate specificities of both TPTs and PPTs from higher plants. Data for TPT and PPT are taken from transport experiments with higher plants (SoTPT, BoPPT) (Kammerer *et al.* 1998).

The results presented in figure 11 show that the TgPT has substrate specificities similar to plant TPTs and PPTs, accepting triose phosphates, PEP and 3-PGA as substrates. Glc6P is only poorly transported by both the TgPT and the plant transporters (Figure 10 and 11), and when the hexose phosphates have to compete with other phosphorylated substrates under *in vivo* conditions they are not transported at all. The transport activity of triose phosphates and 3-PGA are considerable higher for the TgPT than the plant transporters, which can be explained by the apicoplast relying on an indirect transport of energy and reduction power carried out by a shuttle of triose phosphate / 3-PGA.

3.5 Analysis of enzyme kinetics

The kinetic data from the transport experiments were analyzed according to the Michaelis-Menten model to determine apparent K_m and K_i values for the substrates accepted by the TgPT. K_m is an indicator of the affinity that an enzyme has for a given substrate. A low K_m value indicates high affinity to the substrate, and an enzyme that recognizes different substrates will have a different K_m for each substrate.

$V_0 = V_{max} [S] / (K_m + [S])$ Michaelis-Menten equation

The reaction rate (V) increases with increasing substrate concentration, [S], asymptotically approaching the maximum rate (V_{max}). The Michaelis-Menten constant (K_m) is equivalent to the substrate concentration at which the rate of transport is half of V_{max}. To calculate the K_m and V_{max} in a more precise way, the Michaelis-Menten equation can be converted into a linear form by taking the reciprocal of both sides of the equation. This is called the Lineweaver-Burk equation and the method transforms the hyperbolic Michaelis-Menten equation to a linear equivalent, from which the V_{max} and K_m parameters can be determined.

$1 / V_0 = 1 / V_{max} + (K_m / V_{max}) * (1 / [S])$ Lineweaver-Burk equation

Many substrates for enzymes or transporters are not available in a radioactive form. Since they are unlabeled there is no way to directly measure their affinity for the protein. The affinity of the unlabeled substrate for the protein can be determined indirectly by measuring its ability to compete with a radioactive labeled substrate for the protein.

$K_i = K_m [I] / (K_m (app) - K_m)$ Competitive inhibition

To measure the effect of an inhibitor the enzyme velocity is measured at a variety of substrate concentrations in the presence and absence of an inhibitor. In the presence of a competitive inhibitor it takes a higher substrate concentration to achieve the same velocities that were reached in its absence. Although V_{max} can still be reached if sufficient substrate is available, one-half V_{max} requires a higher [S] than before and as a result the K_m value is higher. An inhibitor constant, K_i, similar to the K_m, can be defined and incorporated into the Michaelis-Menten equation (Motulsky 1999).

.

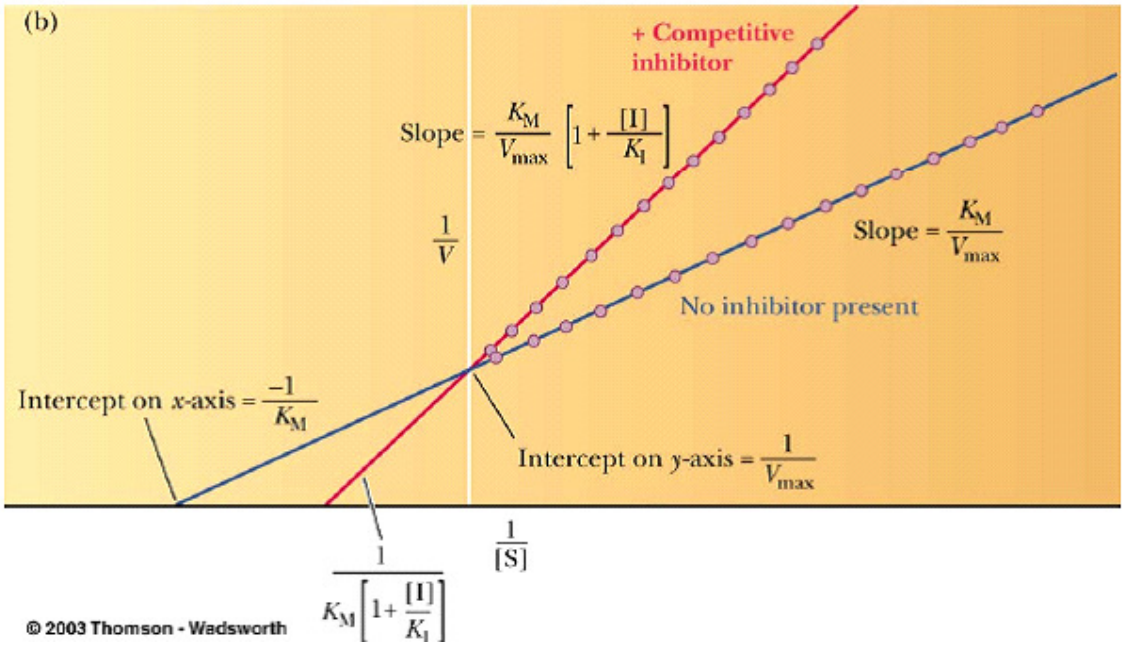

Figure 12: A graphical presentation of the Lineweaver-Burk equation of enzyme kinetics. The Lineweaver-Burk plot provides a useful graphical method for analysis of the Michaelis-Menten equation (Lineweaver and Burk 1934).

In a Lineweaver-Burk plot, K_m is derived from the negative x-axis intercept and V_{max} is obtained from the y-axis intercept (Figure 12). In the presence of a competitive inhibitor, the K_m value will increase due to the ability of the inhibitor to affect the transport of phosphate. The V_{max} value will not change. From the negative x-axis intercept in presence of the competitive inhibitor a K_i value for the competing substrate can be calculated (Motulsky 1999).

3.6 Kinetic constants

The TgPT appears to combine the substrate specificities of both TPTs and PPTs from higher plants, accepting inorganic phosphate, PEP**,** triose phosphates and 3-PGA (Table 6). In order to support the substrate specificity data the apparent kinetic constants were measured for all substrates accepted by the TgPT. To determine the apparent K_m value for inorganic phosphate the transport experiments were repeated using liposomes preloaded with 20 mM inorganic phosphate and different concentrations of [^{32}P]-P_i as external counter exchange substrate.

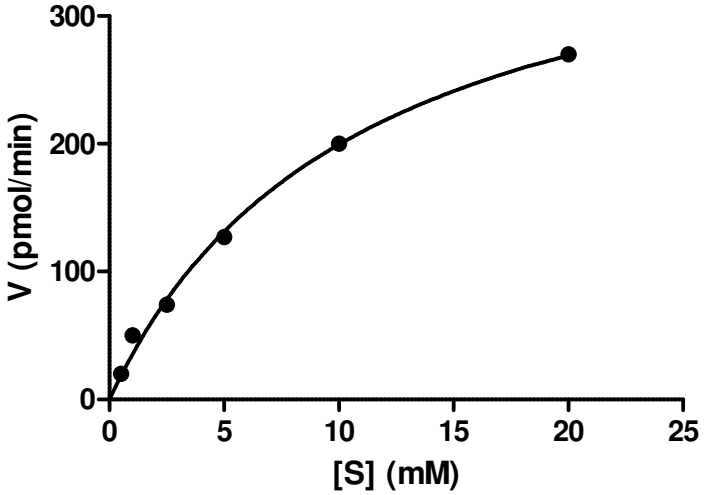

Figure 13: Determination of the Michaelis-Menten constant. The phosphate/phosphate exchange activity measured at different concentrations of inorganic phosphate. Velocity is given as pmol/min and the concentration of substrate is given in mM. The transport activity goes up with increasing substrate concentration. K_m is the substrate concentration where V equals one-half V_{max}.

The phosphate/phosphate counter exchange activity (Figure 13) was used to determine the apparent K_m value of inorganic phosphate. The data were analyzed by a Lineweaver-Burk plot (not shown) to obtain more accurate values for K_m and V_{max}. The Lineweaver-Burke plot increases the precision by linearizing the data**,** and provides a useful graphical method for analysis of the Michaelis-Menten equation. The apparent K_m value for phosphate was determined from several independent experiments.

To facilitate detection of the substrate transport activity, K_m can only be determined for radioactively labeled substrates. For the additional substrates transported by the TgPT binding of a variety of concentrations (0.2 - 20 mM) of inorganic phosphate were measured in absence and presence of the unlabeled substrates to determine apparent K_i values. All liposomes were preloaded with 20 mM P_i.

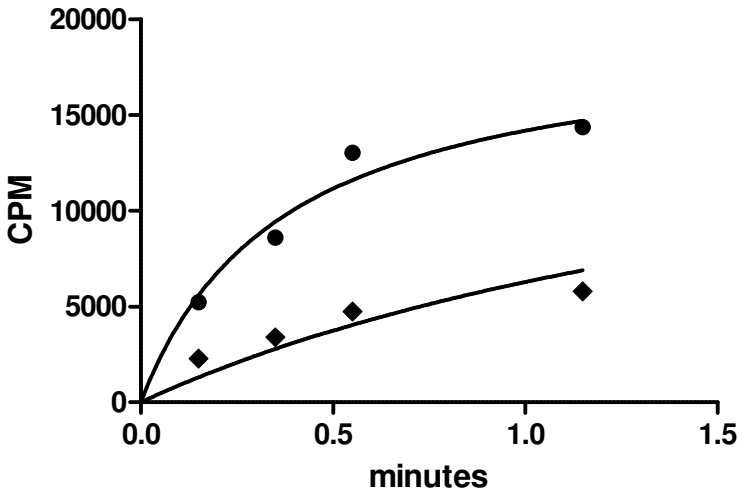

Figure 14: Determination of inhibitor affinities. Transport activity (CPM) of phosphate in absence (●) and presence (♦) of triose phosphate (5 mM) as competitive inhibitor. There is a decrease in the transport rate for phosphate when triose phosphate is present, indicating that triose phosphate is transported by the TgPT and thereby inhibiting transport of phosphate.

The data presented in figure 14 shows the results from a single experiment with 5 mM triose phosphate acting as competitive inhibitor on different concentrations (0.2-2 mM) of inorganic phosphate. With increasing concentrations of substrate the inhibition by triose phosphate decreases. A Lineweaver-Burk plot of the results (not shown) enables determination of the apparent K_i value for triose phosphate (shown in table 7).

The apparent kinetic constants for triose phosphates, PEP and 3-PGA were determined by measuring the enzyme velocity at a variety of phosphate concentrations in the presence and absence of various competitive substrates. The results were analyzed by Lineweaver-Burk plots to determine the apparent K_i values.

Table 7: The apparent K_m and K_i values for various phosphorylated metabolites. The kinetic constants calculated for phosphate (K_m), 3-PGA, triose phosphates and PEP (K_i) by graphical analysis (Lineweaver-Burk).

Substrate	Kinetic constant	TgPT
Phosphate	K_m	1.39 ± 0,28 mM
Triose phosphate	K_i	1.63 ± 0,26 mM
3-PGA	K_i	1.33 ± 0,49 mM
PEP	K_i	1.65 ± 0,52 mM

Data are summarized as the mean ± SE from 4-6 independent experiments

Inorganic phosphate has an apparent K_m value of 1.39 mM (Table 7), which is close to the apparent K_m values of the plant transporters that are ranging from 0.8 to 1.1 mM (Fischer *et al.* 1997, Kammerer *et al.* 1998). The apparent constants for competitive inhibition (K_i) measured for the additional substrates transported by the TgPT are all in the same range as the K_m for phosphate (Table 7), indicating that the transporter is accepting the metabolites equally and thereby are having similar affinity to all of the substrates. The apparent kinetic constants validate the information from the substrate specificity experiments (Table 6), and the TgPT obviously combine the substrate specificities of both TPTs and PPTs from higher plants.

4. Discussion

4.1 The TgPT connects apicoplast and cytosolic metabolic pathways

T. gondii possesses one plastidic membrane protein (TgPT) located in the apicoplast envelope membrane that shows similarity to the plant plastid phosphate translocators (Fleige *et al.* 2007, Karnataki *et al.* 2007). Based on knowledge about the *Plasmodium* genome and the sugar metabolism in *T.gondii,* the proposed function of the TgPT is to transport metabolites between the cytosolic glycolysis and metabolic pathways in the apicoplast (Fleige *et al.* 2007, Roos 2002). In plants the glycolytic pathways localized in the cytosol and the chloroplasts are connected by pPTs transporting phosphorylated intermediates of glycolysis across the inner envelope membrane (Flügge *et al.* 2003). The *T.gondii* genome holds all the glycolytic enzymes as duplicates with the exception of hexokinase and glucose-6-phosphate isomerase (GPI), which are encoded once in the genome. Whereas the cytosol contains a complete set of enzymes for glycolysis, at least three glycolytic isoenzymes are evidently targeted to the apicoplast (Fleige *et al.* 2007). None of the phosphate translocators from algae and higher plants have the ability to transport simultaneously compounds phosphorylated at C-atom 2 (e.g. PEP) and C-atom 3 (e.g. triose phosphates and 3-PGA), respectively (Flügge *et al.* 2003). Higher plants therefore possess up to four different pPT subfamilies with different substrate specificities (Knappe *et al.* 2003). Because *T. gondii* obviously possesses only one plastidic transporter it was proposed that the TgPT possibly was transporting more than one substrate (Fleige *et al.* 2007).

The TgPT is evidently involved in integration of the apicoplast into the cellular metabolism, and a detection of its physiological functions will increase the knowledge about the metabolism of Apicomplexa and might enable the development of new drug targets. In order to determine the role of the apicoplast, the function of the *T. gondii* membrane translocator was analyzed. By heterologous expression of the TgPT gene in yeast and reconstitution of its transport activity in liposomes the substrate specificities of the TgPT were identified. Further, the results were verified by determination of the kinetic constants, K_m and K_i, for substrates accepted by the transporter. Liposomes were preloaded with the different substrates and [^{32}P]-P_i was used as external counter exchange substrate. The transport activities were measured by liquid scintillation counting of [^{32}P] imported into the liposomes at different time points after induction.

In this study, we have demonstrated that the phosphate translocator in *T. gondii* (TgPT) is able to transport triose phosphates, 3-PGA and PEP, but does not possess any transport activity of glucose-6-phosphate (Table 6) or other hexose phosphates (data not shown). The TgPT accepts inorganic phosphate and PEP equally as substrates, having an even higher affinity to triose phosphates and 3-PGA. The apparent kinetic constants for the substrates accepted by the TgPT were determined and they were all in the same range as the K_m for phosphate (Table 7), supporting the substrate specificity data. The substrate specificities of the phosphate translocator in *T.gondii* (this study) was compared with transport activity data from the pPTs from red algae (Linka *et al.* 2008) and higher plants (Kammerer *et al.* 1998) (Table 6). The TgPT showed similarities to both TPTs and PPTs from higher plants combining the transport activity of the two transporters by simultaneously transporting compounds phosphorylated at different C-atoms.

All components needed to shuttle triose phosphates and 3-PGA are expressed in *T. gondii*, namely the cytosolic and plastid isoforms of phosphoglycerate kinase (PGK), glyceraldehyde 3-phosphate dehydrogenase (GAPDH) and triose phosphate isomerase (TPI) (Fleige *et al.* 2007). The shuttle of triose phosphates and 3-PGA results in a net transfer of ATP and NADH from the cytosol to the apicoplast, which is necessary to provide biosynthetic pathways in the apicoplast with energy and reduction power since the apicoplast has no photosynthetic activity (Mazumdar and Striepen 2007). Because apicoplasts lack an oxidative pentose phosphate pathway (OPPP), the GAPDH reaction, together with the pyruvate dehydrogenase (PDH) are the only processes producing reducing equivalents (NADH/NADPH) inside the plastid. The importance of the triose phosphate / 3-PGA shuttle is reflected in the high transport rate of triose phosphates and 3-PGA compared to the plant transporters (Table 7). The red algae *G. sulphuraria* possesses both TPTs and PPTs, but neither of them show any 3-PGA transport activity (Linka *et al.* 2008). Since both NADPH and ATP are produced by photosynthesis in red algae they are most likely not dependent of energy and reduction power acquired from the triose phosphate / 3-PGA shuttle in the same way as the non-photosynthetic *T.gondii*.

The apicoplast, similar to other non-green plastids, is not able to convert 3-PGA into PEP because they lack enolase. 3-PGA produced from triose phosphates is therefore exported to the cytosol, converted into PEP, and then re-imported into the apicoplast for use in the DOXP pathway and fatty acid synthesis. Inside the apicoplast, PEP can be converted by pyruvate kinase to pyruvate, which in turn serves as a substrate for the PDH complex to produce Acetyl-CoA for fatty acid synthesis. The presence of the PDH complex in apicoplasts has important implications for the Acetyl-CoA dependent pathway because it appears to be the only enzyme which can provide the apicoplast with Acetyl-CoA (Fleige *et al.* 2007). In addition, the conversion of pyruvate into Acetyl-CoA produces NADH, which is reduction power required for fatty acid synthesis in non-photosynthetic plastids (Goodman *et al.* 2007).

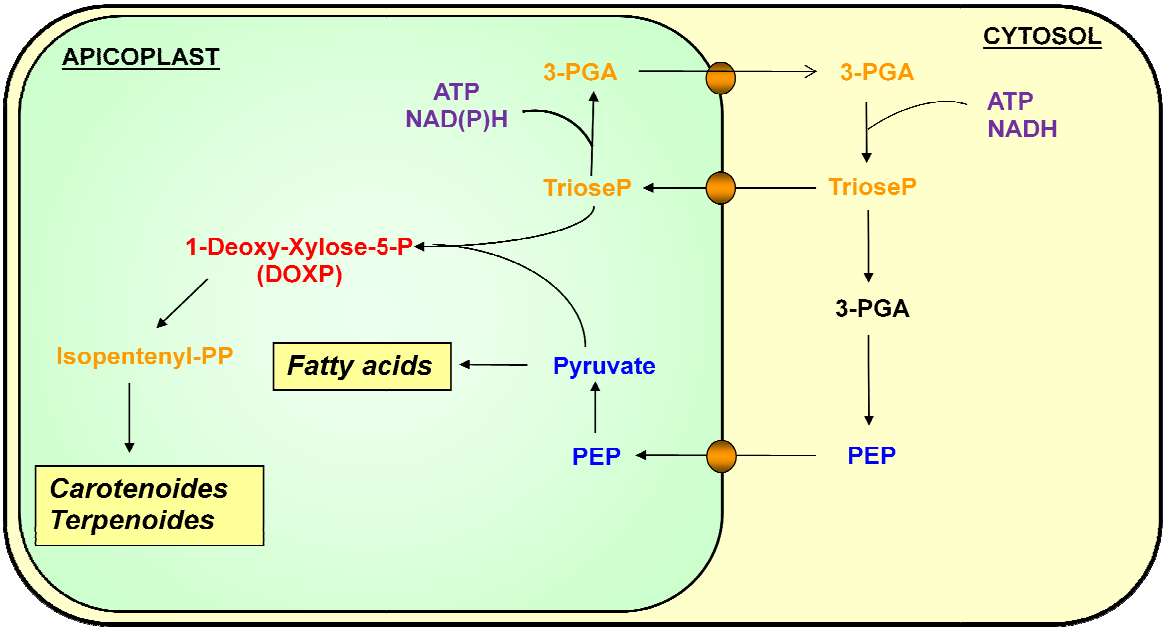

Figure 15: Proposed functions of the TgPT. The shuttle of triose phosphates and 3-PGA results in a net transfer of energy (ATP) and reduction power (NADH) from the cytosol to the apicoplast (Mazumdar and Striepen 2007). The triose phosphates are fed into the DOXP pathway where precursors for isoprenoid biosynthesis are produced. 3-PGA produced from triose phosphate is exported from the apicoplast, converted into PEP in the cytosol and then re-imported. Phosphate is released and pyruvate is fed into the DOXP pathway and fatty acid synthesis (Fleige *et al.* 2007).

Both red algae and *T.gondii* lack any pPTs transporting Glc6P or other hexose phosphates (GPTs) (Linka *et al.* 2008). The GPTs are established only in green algae and higher plants, indicating that the evolution of GPTs is connected to the evolution of starch metabolism (Deschamps *et al.* 2008). In red algae and *T.gondii* the starch synthesis is still localized in the cytosol, but a relocation of the starch synthesis into plastids in green algae made the development of plastid transporters (GPTs) necessary for import of starch precursors (Coppin *et al.* 2005). The absence of Glc6P transport activity in *T. gondii*, in addition to the lack of starch synthesis, can be explained by the lack of a plastid localized glucose-6-phosphate isomerase (GPI). If Glc6P were imported into the apicoplast it would not be able to enter the glycolytic pathway since *T.gondii* possesses only one GPI, which is located in the cytosol (Fleige *et al.* 2007). GPI is an essential enzyme for catabolic glycolysis and anabolic gluconeogenesis that takes part in both the oxidative pentose phosphate pathway (OPPP) and starch synthesis in plants (Grauvogel *et al.* 2007).

4.2 Therapeutic implications

The currently available drugs against diseases caused by the phylum Apicomplexa are often relatively toxic to the host, as most are based on targeting biochemical pathways which are shared between host and parasite (Luzzi and Peto 1993, Salako 1984). The discovery of a relict plastid in apicomplexan parasites (McFadden *et al.* 1996) followed by the detection of metabolic pathways within by the apicoplast and most recently the determination of the substrate specificities of the *T. gondii* phosphate translocator, revealed a new range of drug targets for the treatment of apicomplexan diseases (McFadden and Roos 1999, Ralph *et al.* 2001). By developing treatment directed against any of the metabolic pathways in the apicoplast the parasitic diseases can be controlled without affecting the hosts.

The antimalarial activities of antibiotics were observed first in the late 1940s when animal studies and clinical trials demonstrated that chloramphenicol and tetracyclines had antimalarial properties (Dahl 2008). Treatment with antibiotics has almost no effect on parasite growth during the first intracellular cycle, whereas the parasites die during reinvasion of new host cells. This effect seems to be related to the fact that the likely targets of the antibiotics are primarily essential for replication of the apicoplast, giving rise to apicoplast deficient daughter cells during intracellular division (Wiesner and Jomaa 2007). The antibiotics quinolones and fluoroquinolones are believed to inhibit apicoplast-localized

prokaryotic DNA gyrases, resulting in an arrest of the plastidic DNA replication. The antiparasitic activity of rifampicin is most likely linked to inhibition of the apicoplast RNA polymerase, and numerous anti-bacterial agents are considered to inhibit protein synthesis inside the apicoplast. A common characteristic of most of these antibiotics is a delayed death effect where the parasite remains viable for a prolonged time after drug exposure. It was demonstrated that the plastid genome of *T. gondii* began to degrade in the cycles after antibiotic treatment, linking the effects of antibiotics to the apicoplast (Fichera and Roos 1997).

A recent study has demonstrated that although drugs which interfere with the prokaryotic housekeeping functions of translation, transcription and genome replication lead to apicoplast loss, they do not kill the parasites rapidly, as they permit other apicoplast biochemical processes to proceed. However, parasites treated with metabolic inhibitors that target key enzymes of the apicoplast fatty acid or isoprenoid biosynthetic pathways, have an immediate effect on the parasite (Ramya *et al.* 2007). Both pathways are involved in the production and modification of lipids, and lipid-bound proteins could be required for the parasite-host interaction or the generation of the parasitophorous vacuole, which are essential for successful invasion of new host cells (Ralph *et al.* 2004). During invasion of new host cells, the parasite forms a parasitophorous vacuole that enables an efficient uptake of nutrients and protection against host immune defenses. A breakage of the parasitophorous vacuole membrane (PVM) causes death to the parasites, but the cause is still unclear (Zhao *et al.* 2009).

4.3 Conclusion

Based on our results, the TgPT likely connect the cytosolic metabolism with metabolic pathways in the apicoplast by delivering carbon units for at least two essential biosynthetic pathways, the fatty acid synthesis and the DOXP pathway for isoprenoid synthesis. Additionally, the TgPT contributes an indirect supply of ATP and reduction power to the apicoplast. The pathways for biosynthesis of fatty acids and isoprenoids localized to the apicoplast are known to be essential for survival of the parasites (Jomaa *et al.* 1999, Mazumdar *et al.* 2006). Thus, the transporter delivering substrates to these pathways can be expected to be equally vital for the parasite. Recently, it has been established that a knock-out of the TgPT leads to rapid death of *T. gondii* (Brooks *et al*, submitted), confirming that the phosphate translocator is essential for parasite survival. This knowledge, together with the

determination of the TgPT substrate specificities, the *T. gondii* translocator appears attractive as potential drug target for treatment of parasitic diseases without any delayed effect.

Further genetic and biochemical analysis of the apicoplast should be performed in order to reveal more details about the functions of the organelle. In the search for new drug targets a thoroughly description of the apicoplast metabolism has to be completed. Finding drugs acting without any delay is important as acute infections need to be controlled immediately. Furthermore, the delayed death effect can have implications for development of drug resistance within the apicomplexan parasites (Goodman *et al.* 2007). The cause of the delayed death observed following the loss of apicoplast function is still unknown. With the intention to understand the basis for the delayed death phenotype, pharmacological studies need to be complemented with molecular studies using techniques for genetic manipulation in *Plasmodium* and *Toxoplasma* (Balu and Adams 2007, Mazumdar *et al.* 2006).

5. References

Balu, B. and Adams, J.H. (2007) Advancements in transfection technologies for Plasmodium. *Int J Parasitol*, **37**, 1-10.

Berdoy, M., Webster, J. P., Macdonald, D. W. (2000) Fatal attraction in rats infected with Toxoplasma gondii. *Proc Biol Sci*, **267**, 1591-1594.

Birnboim, H.C. and Doly, J. (1979) A rapid alkaline extraction procedure for screening recombinant plasmid DNA. *Nucl. Acids Res.*, **7**, 1513-1523.

Bowsher, C.G., Boulton, E.L., Rose, J., Nayagam, S. and Emes, M.J. (1992) Reductant for glutamate synthase in generated by the oxidative pentose phosphate pathway in non-photosynthetic root plastids. *The Plant Journal*, **2**, 893-898.

Cai, X., Fuller, A. L., McDougald, L. R., Zhu, G. (2003) Apicoplast genome of the coccidian Eimeria tenella. *Gene*, **321**, 39-46.

Calvin, N.M. and Hanawalt, P.C. (1988) High-efficiency transformation of bacterial cells by electroporation. *J. Bacteriol.*, **170**, 2796-2801.

Cavalier-Smith, T. (1982) The Origins of Plastids. *Biological Journal of the Linnean Society*, **17**, 289-306.

Coppin, A., Varré, J.-S., Lienard, L., Dauvillée, D., Guérardel, Y., Soyer-Gobillard, M., Buléon, A., Ball, S. and Tomavo, S. (2005) Evolution of Plant-Like Crystalline Storage Polysaccharide in the Protozoan Parasite Toxoplasma gondii Argues for a Red Alga Ancestry. *Journal of Molecular Evolution*, **60**, 257-267.

Dahl, E.L., Rosenthal, P. J. (2008) Apicoplast translation, transcription and genome replication: targets for antimalarial antibiotics. *Trends in Parasitology*, **24**, 279-284.

David, S.R., Michael, J.C., Robert, G.K.D., Martin, F., Omar, S.H., Cynthia, Y.H., Jessica, C.K., Michael, K.S. and Boris, S. (2002) Mining the Plasmodium genome database to define organellar function: what does the apicoplast do? *Philosophical Transactions of the Royal Society B: Biological Sciences*, **357**, 35-46.

Deschamps, P., Moreau, H., Worden, A.Z., Dauvillee, D. and Ball, S.G. (2008) Early Gene Duplication Within Chloroplastida and Its Correspondence With Relocation of Starch Metabolism to Chloroplasts. *Genetics*, **178**, 2373-2387.

Disch, A., Schwender, J., Muller, C., Lichtenthaler, H.K. and Rohmer, M. (1998) Distribution of the mevalonate and glyceraldehyde phosphate/pyruvate pathways for isoprenoid biosynthesis in unicellular algae and the cyanobacterium Synechocystis PCC 6714. *Biochemical Journal*, **333**, 381-388.

Eicks, M., Maurino, V., Knappe, S., Flugge, U.-I. and Fischer, K. (2002) The Plastidic Pentose Phosphate Translocator Represents a Link between the Cytosolic and the Plastidic Pentose Phosphate Pathways in Plants. *Plant Physiol.*, **128**, 512-522.

Fast, N.M., Kissinger, J.C., Roos, D.S. and Keeling, P.J. (2001) Nuclear-Encoded, Plastid-Targeted Genes Suggest a Single Common Origin for Apicomplexan and Dinoflagellate Plastids. *Mol Biol Evol*, **18**, 418-426.

Fichera, M.E. and Roos, D.S. (1997) A plastid organelle as a drug target in apicomplexan parasites. *Nature*, **390**, 407-409.

Fischer, K., Kammerer, B., Gutensohn, M., Arbinger, B., Weber, A., Hausler, R.E. and Flugge, U.I. (1997) A New Class of Plastidic Phosphate Translocators: A Putative Link between Primary and Secondary Metabolism by the Phosphoenolpyruvate/Phosphate Antiporter. *Plant Cell*, **9**, 453-462.

Fischer, K. and Weber, A. (2002) Transport of carbon in non-green plastids. *Trends in Plant Science*, **7**, 345-351.

Fleige, T., Fischer, K., Ferguson, D.J.P., Gross, U. and Bohne, W. (2007) Carbohydrate Metabolism in the Toxoplasma gondii Apicoplast: Localization of Three Glycolytic

Isoenzymes, the Single Pyruvate Dehydrogenase Complex, and a Plastid Phosphate Translocator. *Eukaryotic Cell*, **6**, 984-996.

Flügge, U.-I. (1999) Phosphate translocators in plastids. *Annual Review of Plant Physiology and Plant Molecular Biology*, **50**, 27-45.

Flügge, U.I., Fischer, K., Gross, A., Sebald, W., Lottspeich, F. and Eckerskorn, C. (1989) The triose phosphate-3-phosphoglycerate-phosphate translocator from spinach chloroplasts: nucleotide sequence of a full-length cDNA clone and import of the in vitro synthesized precursor protein into chloroplasts. *EMBO J*, **8**, 39-46.

Flügge, U.I., Häusler, R.E., Ludewig, F. and Fischer, K. (2003) Functional genomics of phosphate antiport systems of plastids. *Physiologia Plantarum*, **118**, 475-482.

Foth, B.J., Ralph, S.A., Tonkin, C.J., Struck, N.S., Fraunholz, M., Roos, D.S., Cowman, A.F. and McFadden, G.I. (2003) Dissecting Apicoplast Targeting in the Malaria Parasite Plasmodium falciparum. *Science*, **299**, 705-708.

Funes, S., Davidson, E., Reyes-Prieto, A., Magallon, S., Herion, P., King, M.P. and Gonzalez-Halphen, D. (2002) A Green Algal Apicoplast Ancestor. *Science*, **298**, 2155.

Funes, S., Reyes-Prieto, A., Pérez-Martínez, X. and González-Halphen, D. (2004) On the evolutionary origins of apicoplasts: revisiting the rhodophyte vs. chlorophyte controversy. *Microbes and Infection*, **6**, 305-311.

Gardner, M.J., Hall, N., Fung, E., White, O., Berriman, M., Hyman, R.W., Carlton, J.M., Pain, A., Nelson, K.E., Bowman, S., Paulsen, I.T., James, K., Eisen, J.A., Rutherford, K., Salzberg, S.L., Craig, A., Kyes, S., Chan, M.S., Nene, V., Shallom, S.J., Suh, B., Peterson, J., Angiuoli, S., Pertea, M., Allen, J., Selengut, J., Haft, D., Mather, M.W., Vaidya, A.B., Martin, D.M., Fairlamb, A.H., Fraunholz, M.J., Roos, D.S., Ralph, S.A., McFadden, G.I., Cummings, L.M., Subramanian, G.M., Mungall, C., Venter, J.C., Carucci, D.J., Hoffman, S.L., Newbold, C., Davis, R.W., Fraser, C.M. and Barrell, B. (2002) Genome sequence of the human malaria parasite Plasmodium falciparum. *Nature*, **419**, 498-511.

Goodman, C.D., Su, V. and McFadden, G.I. (2007) The effects of anti-bacterials on the malaria parasite Plasmodium falciparum. *Mol Biochem Parasitol*, **152**, 181-191.

Gould, S.B., Waller, R.F. and McFadden, G.I. (2008) Plastid Evolution. *Annual Review of Plant Biology*, **59**, 491-517.

Grauvogel, C., Brinkmann, H. and Petersen, J. (2007) Evolution of the glucose-6-phosphate isomerase: the plasticity of primary metabolism in photosynthetic eukaryotes. *Mol Biol Evol*, **24**, 1611-1621.

Hager, K., Striepen, B., Tilney, L. and Roos, D. (1999) The nuclear envelope serves as an intermediary between the ER and Golgi complex in the intracellular parasite Toxoplasma gondii. *J Cell Sci*, **112**, 2631-2638.

Hanke, G., Bowsher, C., N Jones, M., Tetlow, I. and Emes, M. (1999) Review article. Proteoliposomes and plant transport proteins. *J. Exp. Bot.*, **50**, 1715-1726.

Harper, J.T. and Keeling, P.J. (2003) Nucleus-Encoded, Plastid-Targeted Glyceraldehyde-3-Phosphate Dehydrogenase (GAPDH) Indicates a Single Origin for Chromalveolate Plastids. *Mol Biol Evol*, **20**, 1730-1735.

He, C.Y., Shaw, M.K., Pletcher, C.H., Striepen, B., Tilney, L.G. and Roos, D.S. (2001) A plastid segregation defect in the protozoan parasite Toxoplasma gondii. *EMBO J*, **20**, 330-339.

Hoffman, C.S. and Winston, F. (1987) A ten-minute DNA preparation from yeast efficiently releases autonomous plasmids for transformation of Escherichia coli. *Gene*, **57**, 267-272.

http://www.piercenet.com/files/WBGuide.pdf Chemiluminescent Western Blotting Technical Guide and Protocols.

Ito, H., Fukuda, Y., Murata, K. and Kimura, A. (1983) Transformation of intact yeast cells treated with alkali cations. *J. Bacteriol.*, **153**, 163-168.

Johnston, M., Flick, J.S. and Pexton, T. (1994) Multiple mechanisms provide rapid and stringent glucose repression of GAL gene expression in Saccharomyces cerevisiae. *Mol. Cell. Biol.*, **14**, 3834-3841.

Jomaa, H., Wiesner, J., Sanderbrand, S., Altincicek, B., Weidemeyer, C., Hintz, M., Rbachova, I., Eberl, M., Zeidler, J., Lichtenthaler, H.K., Soldati, D. and Beck, E. (1999) Inhibitors of the Nonmevalonate Pathway of Isoprenoid Biosynthesis as Antimalarial Drugs. *Science*, **285**, 1573-1576.

Kammerer, B., Fischer, K., Hilpert, B., Schubert, S., Gutensohn, M., Weber, A. and Flugge, U.-I. (1998) Molecular Characterization of a Carbon Transporter in Plastids from Heterotrophic Tissues: The Glucose 6-Phosphate/Phosphate Antiporter. *Plant Cell*, **10**, 105-118.

Karnataki, A., DeRocher, A., Coppens, I., Nash, C., Feagin, J.E. and Parsons, M. (2007) Cell cycle-regulated vesicular trafficking of *Toxoplasma* APT1, a protein localized to multiple apicoplast membranes. *Molecular Microbiology*, **63**, 1653-1668.

Kasahara, M. and Hinkle, P.C. (1977) Reconstitution and purification of the D-glucose transporter from human erythrocytes. *J. Biol. Chem.*, **252**, 7384-7390.

Kim, K. and Weiss, L.M. (2008) Toxoplasma: the next 100 years. *Microbes and Infection*, **10**, 978-984.

Knappe, S., Flugge, U.I. and Fischer, K. (2003) Analysis of the plastidic phosphate translocator gene family in Arabidopsis and identification of new phosphate translocator-homologous transporters, classified by their putative substrate-binding site. *Plant Physiol*, **131**, 1178-1190.

Kohler, S., Delwiche, C.F., Denny, P.W., Tilney, L.G., Webster, P., Wilson, R.J.M., Palmer, J.D. and Roos, D.S. (1997) A Plastid of Probable Green Algal Origin in Apicomplexan Parasites. *Science*, **275**, 1485-1489.

Levine, N.D. (1988) Progress in Taxonomy of the Apicomplexan Protozoa. *Journal of Eurkaryotic Microbiology*, **35**, 518-520.

Lineweaver, H. and Burk, D. (1934) The Determination of Enzyme Dissociation Constants. *Journal of the American Chemical Society*, **56**, 658-666.

Lingelbach, K. and Joiner, K. (1998) The parasitophorous vacuole membrane surrounding Plasmodium and Toxoplasma: an unusual compartment in infected cells. *J Cell Sci*, **111**, 1467-1475.

Linka, M., Jamai, A. and Weber, A.P.M. (2008) Functional Characterization of the Plastidic Phosphate Translocator Gene Family from the Thermo-Acidophilic Red Alga Galdieria sulphuraria Reveals Specific Adaptations of Primary Carbon Partitioning in Green Plants and Red Algae. *Plant Physiol.*, **148**, 1487-1496.

Loddenkotter, B., Kammerer, B., Fischer, K. and Flugge, U.I. (1993) Expression of the Functional Mature Chloroplast Triose Phosphate Translocator in Yeast Internal Membranes and Purification of the Histidine-Tagged Protein by a Single Metal-Affinity Chromatography Step. *Proceedings of the National Academy of Sciences of the United States of America*, **90**, 2155-2159.

Luft, B.J. and Remington, J.S. (1988) AIDS commentary. Toxoplasmic encephalitis. *J Infect Dis*, **157**, 1-6.

Luzzi, G.A. and Peto, T.E. (1993) Adverse effects of antimalarials. An update. *Drug Saf*, **8**, 295-311.

Mazumdar, J. and Striepen, B. (2007) Make It or Take It: Fatty Acid Metabolism of Apicomplexan Parasites. *Eukaryotic Cell*, **6**, 1727-1735.

Mazumdar, J., Wilson, E.H., Masek, K., Hunter, C.A. and Striepen, B. (2006) Apicoplast fatty acid synthesis is essential for organelle biogenesis and parasite survival in Toxoplasma gondii. *Proceedings of the National Academy of Sciences of the United States of America*, **103**, 13192-13197.

McFadden, G. and Gilson, P. (1995) Something borrowed, something green: lateral transfer of chloroplasts by secondary endosymbiosis. *Trends in Ecology & Evolution*, **10**, 12-17.

McFadden, G.I., Reith, M.E., Munholland, J. and Lang-Unnasch, N. (1996) Plastid in human parasites. *Nature*, **381**, 482-482.

McFadden, G.I. and Roos, D.S. (1999) Apicomplexan plastids as drug targets. *Trends in Microbiology*, **7**, 328-333.

Moore, R.B., Obornik, M., Janouskovec, J., Chrudimsky, T., Vancova, M., Green, D.H., Wright, S.W., Davies, N.W., Bolch, C.J.S., Heimann, K., Slapeta, J., Hoegh-Guldberg, O., Logsdon, J.M. and Carter, D.A. (2008) A photosynthetic alveolate closely related to apicomplexan parasites. *Nature*, **451**, 959-963.

Motulsky, H.J. (1999) Curvefit.com. The complete guide to nonlinear regression

Pfefferkorn, E.R., Eckel, M.E. and McAdams, E. (1988) Toxoplasma gondii: in vivo and in vitro studies of a mutant resistant to arprinocid-N-oxide. *Exp Parasitol*, **65**, 282-289.

Ralph, S.A., D'Ombrain, M.C. and McFadden, G.I. (2001) The apicoplast as an antimalarial drug target. *Drug Resistance Updates*, **4**, 145-151.

Ralph, S.A., van Dooren, G.G., Waller, R.F., Crawford, M.J., Fraunholz, M.J., Foth, B.J., Tonkin, C.J., Roos, D.S. and McFadden, G.I. (2004) Tropical infectious diseases: metabolic maps and functions of the Plasmodium falciparum apicoplast. *Nat Rev Microbiol*, **2**, 203-216.

Ramya, T.N., Mishra, S., Karmodiya, K., Surolia, N. and Surolia, A. (2007) Inhibitors of nonhousekeeping functions of the apicoplast defy delayed death in Plasmodium falciparum. *Antimicrob Agents Chemother*, **51**, 307-316.

Reece, R.J. (2004) *Analysis of genes and genomes* Chichester, West Sussex, England ; Hoboken, NJ: John Wiley & Sons.

Romanos, M.A., Scorer, C.A. and Clare, J.J. (1992) Foreign gene expression in yeast: a review. *Yeast*, **8**, 423-488.

Roos, D.S., Crawford, M.J., Donald, R.G.K., Fraunholz, M., Harb, O.S., He, C.Y., Kissinger, J.C., Shaw, M.K., and Striepen, B (2002) Mining the Plasmodium genome database to define organellar function: what does the apicoplast do? *Philosophical Transactions of the Royal Society B: Biological Sciences* **357(1417)**, 35-46.

Roos, D.S., Donald, R.G., Morrissette, N.S. and Moulton, A.L. (1994) Molecular tools for genetic dissection of the protozoan parasite Toxoplasma gondii. *Methods Cell Biol*, **45**, 27-63.

Salako, L.A. (1984) Toxicity and side-effects of antimalarials in Africa: a critical review. *Bull World Health Organ*, **62 Suppl**, 63-68.

Sambrook, P. (2001) *The musculoskeletal system* Edinburgh ; New York: Churchill Livingstone.

Sato, S., Clough, B., Coates, L. and Wilson, R.J.M. (2004) Enzymes for Heme Biosynthesis are Found in Both the Mitochondrion and Plastid of the Malaria Parasite Plasmodium falciparum. *Protist*, **155**, 117-125.

Sullivan, M., Li, J., Kumar, S., Rogers, M.J. and McCutchan, T.F. (2000) Effects of interruption of apicoplast function on malaria infection, development, and transmission. *Molecular and Biochemical Parasitology*, **109**, 17-23.

Surolia, A., Ramya, T.N.C., Ramya, V. and Surolia, N. (2004) 'FAS't inhibition of malaria. *Biochem. J.*, **383**, 401-412.

Suss-Toby, E., Zimmerberg, J. and Ward, G.E. (1996) Toxoplasma invasion: the parasitophorous vacuole is formed from host cell plasma membrane and pinches off via a fission pore. *Proceedings of the National Academy of Sciences of the United States of America*, **93**, 8413-8418.

Switzer, R.C., Merril, C.R. and Shifrin, S. (1979) A highly sensitive silver stain for detecting proteins and peptides in polyacrylamide gels. *Anal Biochem*, **98**, 231-237.

Szoka, F. and Papahadjopoulos, D. (1980) Comparative Properties and Methods of Preparation of Lipid Vesicles (Liposomes). *Annual Review of Biophysics and Bioengineering*, **9**, 467-508.

Tenter, A.M., Heckeroth, A.R. and Weiss, L.M. (2000) Toxoplasma gondii: from animals to humans. *International Journal for Parasitology*, **30**, 1217-1258.

Ton, V.-K. and Rao, R. (2004) Functional expression of heterologous proteins in yeast: insights into Ca2+ signaling and Ca2+-transporting ATPases. *Am J Physiol Cell Physiol*, **287**, C580-589.

Towbin, H., Staehelin, T. and Gordon, J. (1979) Electrophoretic transfer of proteins from polyacrylamide gels to nitrocellulose sheets: procedure and some applications. *Proceedings of the National Academy of Sciences of the United States of America*, **76**, 4350-4354.

Trape, J.-F., Pison, G., Spiegel, A., Enel, C. and Rogier, C. (2002) Combating malaria in Africa. *Trends in Parasitology*, **18**, 224-230.

Waller, R.F., Keeling, P.J., Donald, R.G., Striepen, B., Handman, E., Lang-Unnasch, N., Cowman, A.F., Besra, G.S., Roos, D.S. and McFadden, G.I. (1998) Nuclear-encoded proteins target to the plastid in Toxoplasma gondii and Plasmodium falciparum. *Proc Natl Acad Sci U S A*, **95**, 12352-12357.

Waller, R.F. and McFadden, G.I. (2005) The apicoplast: a review of the derived plastid of apicomplexan parasites. *Curr Issues Mol Biol*, **7**, 57-79.

Waller, R.F., Ralph, S.A., Reed, M.B., Su, V., Douglas, J.D., Minnikin, D.E., Cowman, A.F., Besra, G.S. and McFadden, G.I. (2003) A type II pathway for fatty acid biosynthesis presents drug targets in Plasmodium falciparum. *Antimicrob Agents Chemother*, **47**, 297-301.

Wiesner, J. and Jomaa, H. (2007) Isoprenoid biosynthesis of the apicoplast as drug target. *Current Drug Targets*, **8**, 3-13.

Wiesner, J., Ortmann, R., Jomaa, H., Schlitzer, M. (2003) New Antimalarial Drugs. *Angewandte Chemie International Edition*, **42**, 5274-5293.

Wilson, K. and Walker, J.M. (2000) *Principles and techniques of practical biochemistry* 5th edn. Cambridge ; New York: Cambridge University Press.

Wilson, R.J.M., Denny, P.W., Preiser, P.R., Rangachari, K., Roberts, K., Roy, A., Whyte, A., Strath, M., Moore, D.J., Moore, P.W. and Williamson, D.H. (1996) Complete Gene Map of the Plastid-like DNA of the Malaria ParasitePlasmodium falciparum. *Journal of Molecular Biology*, **261**, 155-172.

Zhao, Y.O., Khaminets, A., Hunn, J.P. and Howard, J.C. (2009) Disruption of the Toxoplasma gondii parasitophorous vacuole by IFNgamma-inducible immunity-related GTPases (IRG proteins) triggers necrotic cell death. *PLoS Pathog*, **5**, e1000288.

Appendix I

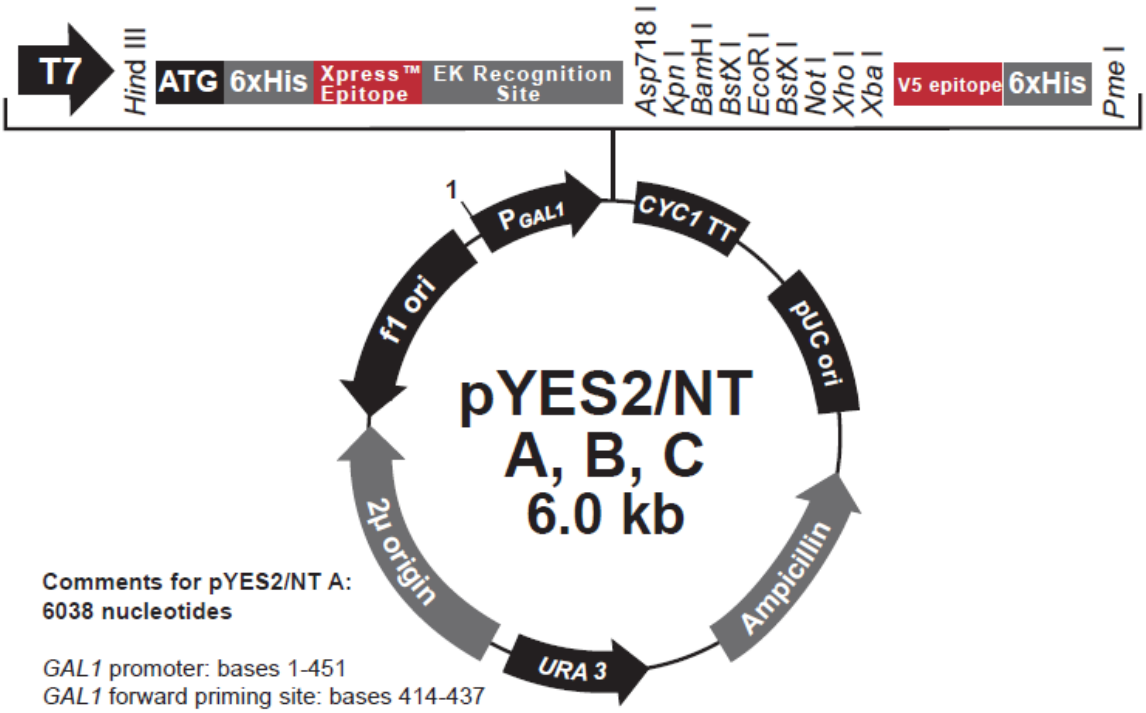

Comments for pYES2/NT A:
6038 nucleotides

GAL1 promoter: bases 1-451
GAL1 forward priming site: bases 414-437
T7 promoter/priming site: bases 475-494
ATG initiation codon: bases 510-512
Polyhistidine (6xHis) region: bases 522-539
Xpress™ epitope: bases 579-602
Enterokinase (EK) recognition site: bases 588-602
Multiple cloning site: bases 602-669
V5 epitope: bases 682-723
Polyhistidine (6xHis) region: bases 733-750
CYC1 transcription termination signal: 783-1036
CYC1 reverse priming site: bases 800-818
pUC origin: bases 1220-1893
Ampicillin resistance gene: bases 2038-2898 (complementary strand)
URA3 gene: bases 2916-4023 (complementary strand)
2µ origin: bases 4027-5498
f1 origin: bases 5566-6021 (complementary strand)

Figure 16: Map of the pYES/NT vector (Invitrogen)

Appendix II

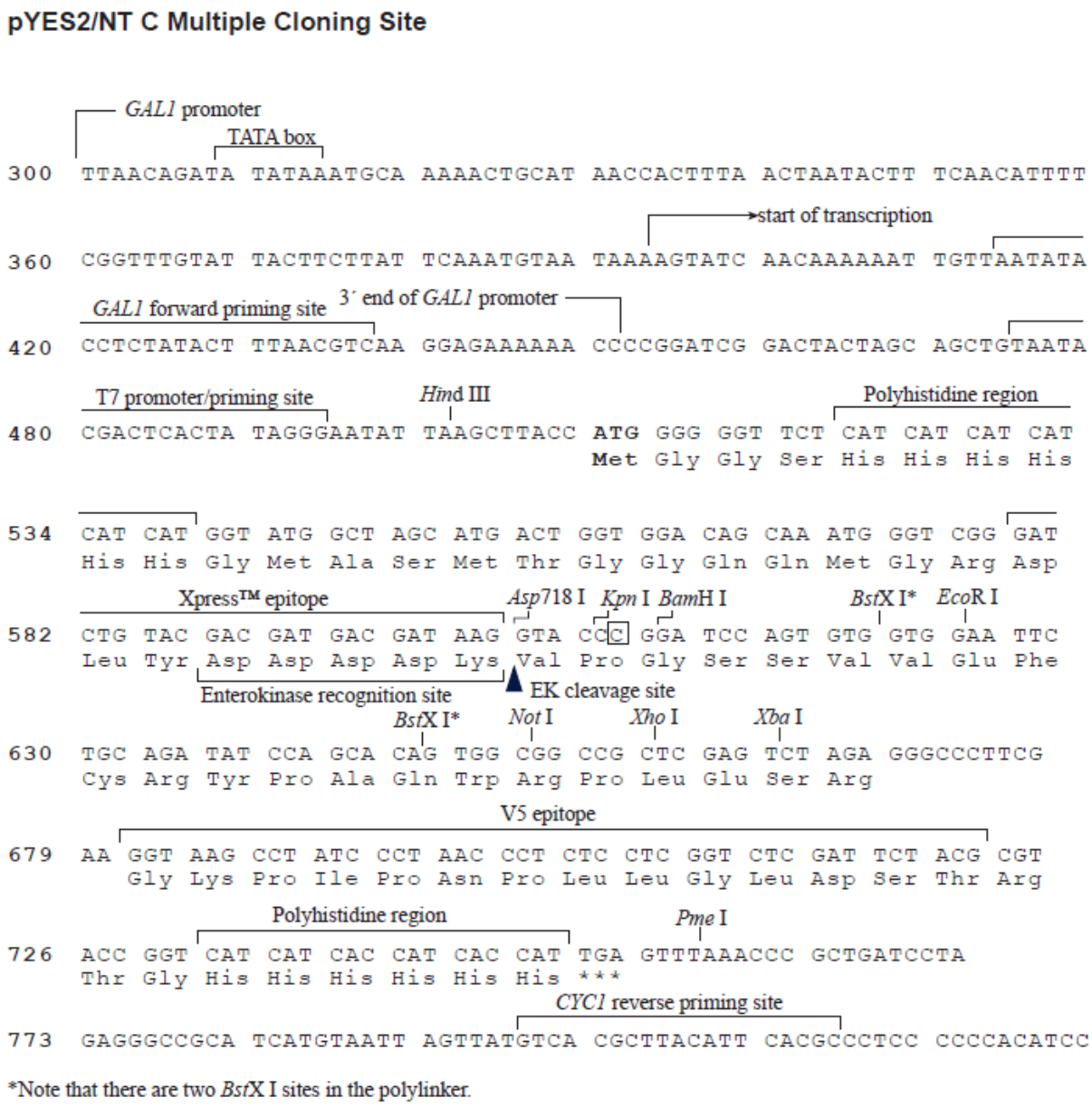

*Note that there are two *Bst*X I sites in the polylinker.

Figure 17: The sequence of the pYES/NT vector (Invitrogen)